Inorg. Chem. **2007**, *46*, 3322–3335

Syntheses, Characterization, and Dioxygen Reactivities of Cu(I) Complexes with *cis*,*cis*-1,3,5-Triaminocyclohexane Derivatives: A $Cu(III)_2O_2$ Intermediate Exhibiting Higher C–H Activation

Yuji Kajita,[†] Hidekazu Arii,[†] Takahiro Saito,[†] Yamato Saito,[†] Shigenori Nagatomo,[‡] Teizo Kitagawa,[‡] Yasuhiro Funahashi,[†] Tomohiro Ozawa,[†] and Hideki Masuda*[,†]

Graduate School of Engineering, Nagoya Institute of Technology, Showa-ku, Nagoya 466-8555, Japan, and Center of Integrative Bioscience, Okazaki National Research Institutes, Myodaiji, Okazaki 444-8585, Japan

Received November 19, 2006

Six Cu(I) complexes with *cis*,*cis*-1,3,5-triaminocyclohexane derivatives (R_3CY, R = Et, iBu, and Bn), $[Cu(MeCN)(Et_3CY)]SbF_6$ (**1**), $[Cu(MeCN)(iBu_3CY)]SbF_6$ (**2**), $[Cu(MeCN)(Bn_3CY)]SbF_6$ (**3**), $[Cu(CO)(Et_3CY)]SbF_6$ (**4**), $[Cu(CO)(iBu_3CY)]SbF_6$ (**5**), and $[Cu(CO)(Bn_3CY)]SbF_6$ (**6**), were prepared to probe the ability of copper complexes to effectively catalyze oxygenation reactions. The complexes were characterized by elemental analysis, electrochemical and X-ray structure analyses, electronic absorption spectroscopy, IR spectroscopy, ^{1}H NMR spectroscopy, and ESI mass spectrometry. The crystal structures of **1**–**3** and **6** and the CO stretching vibrations (ν_{CO}) of **4**–**6** demonstrate that the ability of R_3CY to donate electron density to the Cu(I) atom is stronger than that of the previously reported ligands, 1,4,7-triazacyclononane (R_3TACN) and 1,4,7-triazacyclodecane (R_3TACD). Reactions of complexes **1**–**3** with dioxygen in THF or CH_2Cl_2 at –105 to –80 °C yield bis(μ-oxo)dicopper(III) complexes **7**–**9** as intermediates as confirmed by electronic absorption spectroscopy and resonance Raman spectroscopy. The Cu–O stretching vibrations, ν(Cu–O) for **7** ($^{16}O_2$: 553, 581 cm^{-1}and $^{18}O_2$: 547 cm^{-1}) and **8** ($^{16}O_2$: 571 cm^{-1} and $^{18}O_2$: 544 cm^{-1}), are observed in a lower energy region than previously reported for bis(μ-oxo) complexes. The decomposition rates of complexes **7**–**9** in THF at –90 °C are 2.78×10^{-4} for **7**, 8.04×10^{-4} for **8**, and 3.80×10^{-4} s^{-1} for **9**. The decomposition rates of **7** and **8** in CH_2Cl_2 were 5.62×10^{-4} and 1.62×10^{-3} s^{-1}, respectively, and the thermal stabilities of **7**–**9** in CH_2Cl_2 are lower than the values measured for the complexes in THF. The decomposition reactions obeyed first-order kinetics, and the H/D isotope experiments for **8** and **9** indicate that the N-dealkylation reaction is the rate-determining step in the decomposition processes. On the other hand, the decomposition reaction of **7** in THF results in the oxidation of THF (acting as an exogenous substrate) to give 2-hydroxy tetrahydrofuran and γ-butyrolactone as oxidation products. Detailed investigation of the N-dealkylation reaction for **8** by kinetic experiments using N–H/D at –90 °C showed a kinetic isotope effect of 1.25, indicating that a weak electrostatic interaction between the N–H hydrogen and μ-oxo oxygen contributes to the major effect on the rate-determining step of N-dealkylation. X-ray crystal structures of the bis(μ-hydroxo)dicopper(II) complexes, $[Cu_2(OH)_2(Et_3CY)_2](CF_3SO_3)_2$ (**10**), $[Cu_2(OH)_2(iBu_3CY)_2](CF_3SO_3)_2$ (**11**), and $[Cu_2(OH)_2(Bn_3CY)_2](ClO_4)_2$ (**12**), which have independently been prepared as the final products of bis(μ-oxo)dicopper(III) intermediates, suggest that an effective interaction between N–H and μ-oxo in the $Cu(III)_2(\mu\text{-}O)_2$ core may enhance the oxidation ability of the metal–oxo species.

Introduction

Investigations of the structures and reactivities of dicopper(I) complexes is a worthy endeavor from the viewpoint of understanding of the active intermediate species of O_2 catalyzed by Cu-containing oxidases and synthetic catalysis.[1–5] Several dicopper−oxygen model complexes have been synthesized and characterized by spectroscopic and structural studies.[6–16] Among many studies of dicopper−oxygen spe-

* E-mail: masuda.hideki@nitech.ac.jp. Tel.: +81-52-735-5228. Fax: +81-52-735-5209.
[†] Nagoya Institute of Technology.
[‡] Okazaki National Research Institutes.

(1) Karlin, K. D.; Tyeklár, Z., Eds. *Bioinorganic Chemistry of Copper*; Chapman and Hall: New York, 1993.
(2) Solomon, E. I.; Baldwin, M. J.; Lowery, M. D. *Chem. Rev.* **1992**, *92*, 521−542.

10.1021/ic062206s CCC: $37.00
Published on Web 03/20/2007

cies, a bis(μ-oxo)dicopper(III) complex, first discovered by Tolman and co-workers, has been noted as a possible intermediate in oxidation reactions catalyzed by dicopper enzymes.[9,17−23] Subsequently, many reports concerning the reactivities of the bis(μ-oxo)dicopper(III) complex have arisen. Such reactivities include decomposition reactions accompanied by N-dealkylation,[24,25] control of interconversion between a bis(μ-oxo)dicopper complex and a $-\mu$-η^2:η^2-peroxodicopper complex depending on various counter anions, solvents, and alkyl substituents,[26−30] and the oxidation/oxygenation reactivities of many exogenous substrates.[31−38]

Chart 1

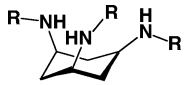

R = Et (Et_3CY)
= iBu (iBu_3CY)
= Bn (Bn_3CY)

Furthermore, this high-valent dicopper(III) species has been demonstrated to be capable of hydroxylation of an aromatic hydrocarbon.[39] The determination of the oxidation mechanism of the bis(μ-oxo)dicopper(III) complex may provide useful insights that lead to a greater understanding of biological reactions that also may be applicable to the development of industrial oxidation catalysts.

We also previously reported that the bis(μ-oxo)dicopper complex with *cis*,*cis*-1,3,5-triaminocyclohexane, which has three isobutyl (iBu) group substituents on the amine nitrogen atoms (Chart 1), decomposed at room temperature and was accompanied by hydroxylation of an β-methine carbon that has a relatively strong C−H bond.[40] This finding suggests the possibility that the high-valent oxo species may be a powerful catalyst for oxidation of exogenous substrates. Although some reports have been published, the mechanisms of the unique oxygenation reaction catalyzed by the bis(μ-oxo)dicopper(III) species with *cis*,*cis*-1,3,5-triaminocyclohexane derivatives have not yet been clarified.

In this paper, we report the syntheses, characterization, and oxygenation reactivities of Cu(I) complexes with triaminocyclohexane derivative ligands R_3CY (R = Et, iBu, and Bn), which have a higher binding ability for copper and stabilize the coordination structure with three rigid six-membered chelate rings constrained by the cyclohexane framework. X-ray crystallography and various spectroscopic methods were used to characterize the structures of the complexes. The thermal stabilities and reactivities of three bis(μ-oxo)dicopper(III) complexes derived from the Cu(I) complexes with dioxygen are drastically affected by the N-alkyl substituents. Interestingly, the bis(μ-oxo)dicopper(III) complex with the Et_3CY ligand, $[Cu_2(\mu\text{-oxo})_2(Et_3CY)_2]^{2+}$, demonstrates a unique oxidization of THF without the occurrence of a ligand decomposition reaction such as N-dealkylation. The attractive interaction between μ-oxo oxygen and H atoms of the secondary amine nitrogens of the R_3CY ligand appear to induce the promotion of a higher reactivity of the μ-oxo oxygen.

Experimental Procedures

Materials and Methods. All reagents used were of the highest grade available and were used without further purification. 1,3,5-

(3) Solomon, E. I.; Sundaram, U. M.; Machonkin, T. E. *Chem. Rev.* **1996**, *96*, 2563−2606.
(4) Gerdemann, C.; Eicken, C.; Krebs, B. *Acc. Chem. Res.* **2002**, *35*, 183−191.
(5) Solomon, E. I.; Chen, P.; Metz, M.; Lee, S.-K.; Palmer, A. E. *Angew. Chem., Int. Ed.* **2001**, *40*, 4570−4590.
(6) Tyeklár, Z.; Karlin, K. D. *Acc. Chem. Res.* **1989**, *22*, 241−248.
(7) Kitajima, N.; Moro-oka, Y. *Chem. Rev.* **1994**, *94*, 737−757.
(8) Karlin, K. D.; Kaderli, S.; Zuberbühler, A. D. *Acc. Chem. Res.* **1997**, *30*, 139−147.
(9) Tolman, W. B. *Acc. Chem. Res.* **1997**, *30*, 227−237.
(10) Holland, P. L.; Tolman, W. B. *Coord. Chem. Rev.* **1999**, *190−192*, 855−869.
(11) Schindler, S. *Eur. J. Inorg. Chem.* **2000**, 2311−2326.
(12) Blackman, A. G.; Tolman, W. B. *Struct. Bonding (Berlin)* **2000**, *97*, 179−211.
(13) Gamez, P.; Koval, I. A.; Reedijk, J. *Dalton Trans.* **2004**, 4079−4088.
(14) Mirica, L. M.; Ottenwaelder, X.; Stack, T. D. P. *Chem. Rev.* **2004**, *104*, 1013−1045.
(15) Lewis, E. A.; Tolman, W. B. *Chem. Rev.* **2004**, *104*, 1047−1076.
(16) Komiyama, K.; Furutachi, H.; Nagatomo, S.; Hashimoto, A.; Hayashi, H.; Fujinami, S.; Suzuki, M.; Kitagawa, T. *Bull. Chem. Soc. Jpn.* **2004**, *77*, 59−72.
(17) Mahapatra, S.; Halfen, J. A.; Wilkinson, E. C.; Pan, G.; Cramer, C. J.; Que, L., Jr.; Tolman, W. B. *J. Am. Chem. Soc.* **1995**, *117*, 8865−8866.
(18) Halfen, J. A.; Mahapatra, S.; Wilkinson, E. C.; Kaderli, S.; Young, V. G., Jr.; Que, L., Jr.; Zuberbühler, A. D.; Tolman, W. B. *Science* **1996**, *271*, 1397.
(19) Mahapatra, S.; Halfen, J. A.; Wilkinson, E. C.; Pan, G.; Wang, X.; Young, V. G., Jr.; Cramer, C. J.; Que, L., Jr.; Tolman, W. B. *J. Am. Chem. Soc.* **1996**, *118*, 11555−11574.
(20) Mahadevan, V.; Hou, Z.; Cole, A. P.; Root, D. E.; Lal, T. K.; Solomon, E. I.; Stack, T. D. P. *J. Am. Chem. Soc.* **1997**, *119*, 11996−11997.
(21) Itoh, S.; Taki, M.; Nakao, H.; Holland, P. L.; Tolman, W. B.; Que, L., Jr.; Fukuzumi, S. *Angew. Chem., Int. Ed.* **2000**, *39*, 398−400.
(22) Hayashi, H.; Fujinami, S.; Nagatomo, S.; Ogo, S.; Suzuki, M.; Uehara, A.; Watanabe, Y.; Kitagawa, T. *J. Am. Chem. Soc.* **2000**, *122*, 2124−2125.
(23) Cole, A. P.; Mahadeva, V.; Milica, L. M.; Ottenwaelder, X.; Stack, T. D. P. *Inorg. Chem.* **2005**, *44*, 7345−7364.
(24) Mahapatra, S.; Halfen, J. A.; Tolman, W. B. *J. Am. Chem. Soc.* **1996**, *118*, 11575−11586.
(25) Shearer, J.; Zhang, C. X.; Hatcher, L. Q.; Karlin, K. D. *J. Am. Chem. Soc.* **2003**, *125*, 12670−12671.
(26) Cahoy, J.; Holland, P. L.; Tolman, W. B. *Inorg. Chem.* **1999**, *38*, 2161−2168.
(27) Mahadevan, V.; Henson, M. J.; Solomon, E. I.; Stack, T. D. P. *J. Am. Chem. Soc.* **2000**, *122*, 10249−10250.
(28) Stack. T. D. P. *Dalton Trans.* **2003**, *10*, 1881−1889.
(29) Liang, H.-C.; Henson, M. J.; Hatcher, L. Q.; Vance, M. A.; Zhang, C. X.; Lahti, D.; Kaderli, S.; Sommer, R. D.; Rheingold, A. L.; Zuberbühler, A. D.; Solomon, E. I.; Karlin, K. D. *Inorg, Chem.* **2004**, *43*, 4115−4117.
(30) Lanying, Q. H.; Michael, A. V.; Narducci Sarjeant, A. A.; Solomon, E. I.; Karlin, K. D. *Inorg. Chem.* **2006**, *45*, 3004−3013.
(31) Mahadevan, V.; Dubois, J. L.; Hedman, B.; Hodgson, K. O.; Stack, T. D. P. *J. Am. Chem. Soc.* **1999**, *121*, 5583−5584.
(32) Taki, M.; Itoh, S.; Fukuzumi, S. *J. Am. Chem. Soc.* **2001**, *123*, 6203−6204.
(33) Zhang, C. X.; Liang, H.-C.; Kim, E.-i.; Shearer, J.; Helton, M. E.; Kim, E.; Kaderli, S.; Incarvito, C. D.; Zuberbühler, A. D.; Rheingold, A. L.; Karlin, K. D. *J. Am. Chem. Soc.* **2003**, *125*, 634−635.
(34) Taki, M.; Itoh, S.; Fukuzumi, S. *J. Am. Chem. Soc.* **2002**, *124*, 998−1002.
(35) Kaizer, J.; Pap, J.; Speier, G.; Párkányi, L. *Eur. J. Inorg. Chem.* **2004**, 2253−2259.
(36) Pavlova, S. V.; Chen, K. H.-C.; Chan, S. I. *Dalton Trans.* **2004**, 3261−3272.
(37) Shearer, J.; Zhang, C. X.; Zakharov, L. N.; Rheingold, A. L.; Karlin, K. D. *J. Am. Chem. Soc.* **2005**, *127*, 5469−5483.
(38) Mirica, L. M.; Vance, M.; Rudd, D. J.; Hedman, B.; Hodgson, K. O.; Solomon, E. I.; Stack, T. D. P. *Science* **2005**, *208*, 1890−1892.
(39) Holland, P. L., Rodgers, K. R.; Tolman, W. B. *Angew. Chem., Int. Ed.* **1999**, *38*, 1139−1142.
(40) Arii, H.; Saito, Y.; Nagatomo, S.; Kitagawa, T.; Funahashi, Y.; Jitsukawa, K.; Masuda, H. *Chem. Lett.* **2003**, 156−157.

cis,cis-Triaminocyclohexane-*N,N′N″*-tri-*p*-toluenesulfonyl amide,[41] *d*-isobutylaldehyde ($(CH_3)_2CHCDO$),[42] $H_3CY \cdot 3HCl$ (*cis,cis*-1,3,5-triaminocyclohexane trihydrochloride), and R_3CY ligands (R = Et, *N,N′N″*-triethyl-1,3,5-*cis,cis*-triaminocyclohexane; R = iBu, *N,N′N″*-triisobutyl-1,3,5-*cis,cis*-triaminocyclohexane; and R = Bn, *N,N′N″*-tribenzyl-1,3,5-*cis,cis*-triaminocyclohexane)[40,43] were synthesized according to the previously reported methods. ***Caution!*** *Perchlorate salts of metal complexes with organic ligands are potentially explosive. Only small amounts of material should be prepared and handled with great care.*

Syntheses of *d*-Derivatives of *cis,cis*-1,3,5-Triaminocyclohexane Ligands. *N,N′N″*-Triethyl(d_5)-1,3,5-*cis,cis*-triaminocyclohexane-*N,N′N″*-tri-*p*-toluenesulfonyl Amide (d_{15}-Et_3Ts_3CY). Na (0.24 g, 1.04×10^{-2} mol) and 1,3,5-*cis,cis*-triaminocyclohexane-*N,N′N″*-tri-*p*-toluenesulfonyl amide (1.00 g, 1.69×10^{-3} mol) were dissolved in 20 mL of dry EtOH with stirring for 30 min. The solvent was removed using a rotary evaporator to obtain a white solid, which was dissolved in dry DMF (30 mL) and to which d_5-EtBr (1.5 mL) was added. The resulting solution was heated to 90 °C and stirred for 20 h. After cooling at room temperature, the solution was added to a concentrated NH_4OH/H_2O solution (30 mL), which was stirred for 1 h. The solvent was removed using a high-vacuum rotary evaporator. The residue was taken up in EtOAc (200 mL), washed with a saturated NaCl solution (50 mL), dried over $MgSO_4$, and concentrated to obtain a pale yellow oil. The pure product was isolated by column chromatography on silica gel, eluting with $CHCl_3$ (yield 79%). FTIR data [KBr, ν (cm^{-1})]: 3278 (N−H), 3029 (aromatic C−H), 2944, 2870 (aliphatic C−H), 2230, 2070 (C−D), 1598, 1494 (aromatic ring). ^1H NMR (δ (ppm vs Me_4Si)) in $CDCl_3$: 7.65 (d, 6H), 7.29 (d, 6H), 3.57 (m, 3H), 2.43 (s, 9H), 1.62 (d, 3H), 1.26 (q, 3H). ESI-TOF/MS data: *m/z* 692 $[M + H]^+$.

***N,N′,N″*-Triethyl(d_{15})-1,3,5-*cis,cis*-triaminocyclohexane (d_{15}-Et_3CY).** To acetic anhydride (7.5 mL) cooled in an ice bath was added concentrated HBr (14 mL). After stirring at room temperature for 18 h, Et_3Ts_3CY (0.9 g, 1.3 mmol) was added to the solution. The resulting suspension was refluxed for 24 h until the solution turned dark reddish-brown. The solution was then evaporated to leave a dark solid, which was dissolved in H_2O (10 mL) and extracted with Et_2O (3 × 20 mL). The aqueous solution layer was filtered and concentrated to ca. 5 mL. The residue was dissolved in EtOH (100 mL), and an equal amount of Et_2O was added to precipitate the product. The white suspension was cooled at 0 °C for 6 h, and then the solid d_{15}-$Et_3CY \cdot 3HBr$ was collected, washed with Et_2O, and dried under vacuum (yield 64%).

The salt d_{15}-$Et_3CY \cdot 3HBr$ (0.4 g, 0.85 mmol) was dissolved in H_2O (15 mL) containing NaOH (0.2 g, 5.1 mmol) to obtain a clear solution. The aqueous solution was extracted with $CHCl_3$ (3 × 15 mL), and the organic layers were collected, dried over dry Mg_2SO_4, and filtered. The solvent was removed by rotary evaporator to leave a colorless oil (yield 79%). FTIR data [KBr, ν (cm^{-1})]: 3267 (N−H), 2923 (aliphatic C−H), 2219, 2069 (C−D). ^1H NMR (δ (ppm vs Me_4Si)) in $CDCl_3$: 2.55 (t, 3H), 2.17 (d, 3H), 0.87 (q, 3H). ESI-TOF/MS data: *m/z* 229 $[M + H]^+$.

***N,N′,N″*-Trisobutyl(d_2)-1,3,5-*cis,cis*-triaminocyclohexane (d_6-iBu_3CY).** To a stirred solution of $H_3CY \cdot 3HBr$ (2.0 g, 5.4 mmol) in H_2O (10 mL) containing NaOH (0.695 g, 16.1 mmol) was added a solution of *d*-isobutylaldehyde ($(CH_3)_2CHCDO$, 1.2 g, 16.5 mmol) in Et_2O (10 mL), which was then stirred for 18 h. The solution was separated into two layers, and the aqueous solution layer was extracted with Et_2O (3 × 10 mL). The organic layers were collected, washed with a saturated salt solution, dried over Mg_2SO_4, and filtered. The solvent was removed using a rotary evaporator to obtain a white solid, which was dissolved in dry MeOH (20 mL). $NaBD_4$ (0.23 g, 5.4 mmol) was added to the solution. After the reaction mixture was stirred for 6 h at room temperature, 10 mL of 6 N HCl was slowly added to the solution. The solvent was removed under reduced pressure, and a yellow oil product was obtained. The product was dissolved in 15 mL of 10% K_2CO_3 solution, and the aqueous solution was extracted with $CHCl_3$ (3 × 15 mL). The organic layers were collected, washed with a saturated salt solution, dried over Mg_2SO_4, filtered, and rotary evaporated to leave a yellow oil (yield 83%). FTIR data [KBr, ν (cm^{-1})]: 2956, 2868 (aliphatic C−H), 2176, 2054 (C−D). ^1H NMR (δ (ppm vs Me_4Si)) in $CDCl_3$: 2.49 (t, 3H), 2.16 (d, 3H), 1.70 (m, 3H), 0.94 (d, 18H), 0.80 (m, 3H). ESI-TOF/MS data: *m/z* 304 $[M + H]^+$.

***N,N′,N″*-Trideutero-*N,N′,N″*-triisobutyl-1,3,5-*cis,cis*-triaminocyclohexane (Nd_3-iBu_3CY).** To a $CDCl_3$ (3 mL) solution of iBu_3CY (0.5 g, 1.68 mmol) was added D_2O (1 mL), and the resulting solution was stirred for 30 min. The solvent was removed under reduced pressure, and a pale yellow oil was obtained. This operation was repeated 5 times (yield 68%). FTIR [KBr, ν (cm^{-1})]: 2956, 2930, 2900, 2869 (aliphatic C−H). ^1H NMR (δ (ppm vs Me_4Si)) in $CDCl_3$: 2.53 (t, 3H), 2.45 (d, 6H), 2.15 (d, 3H), 1.72 (m, 3H), 0.96 (m, 3H), 0.91 (d, 18H). ESI-TOF/MS data: *m/z* 300 $[M]^+$.

***N,N′,N″*-Tribenzyl(d_2)-1,3,5-*cis,cis*-triaminocyclohexane (d_6-Bn_3CY).** d_6-Bn_3CY was synthesized by the same method as d_6-iBu_3CY using *d*-benzaldehyde (C_6H_5CDO) in place of *d*-isobutylaldehyde (yield 84%). FTIR [KBr, ν (cm^{-1})]: 3295 (N−H), 3083, 3057, 3023 (aromatic C−H), 2927, 2899, 2853 (aliphatic C−H), 2068 (C−D), 1610, 1495 (aromatic ring). ^1H NMR (δ (ppm vs Me_4Si)) in $CDCl_3$: 7.33−7.24 (m, 15H), 2.56 (t, 3H), 2.24 (d, 3H), 0.98 (q, 3H). ESI-TOF/MS data: *m/z* 405 $[M + H]^+$.

Syntheses of Copper Complexes. The bis(μ-hydroxo)dicopper(II) complexes were prepared under air, and the preparations of copper(I) complexes were performed under Ar in a glove box.

$[Cu(MeCN)(Et_3CY)]SbF_6$ (1). A THF solution (2 mL) of $[Cu(MeCN)_4]SbF_6$ (122 mg, 2.60×10^{-1} mmol) was added to a THF solution (2 mL) of Et_3CY (70.4 mg, 3.30×10^{-1} mmol). The mixture was stirred for 1 h. After adding 5 mL of diethylether, the solution was left standing for a few days to obtain colorless crystals (yield 77%). Anal. Calcd. for $C_{14}H_{30}F_6CuN_4Sb$: C, 30.37; H, 5.46; N, 10.12. Found: C, 30.36; H, 5.44; N, 9.99. FTIR [KBr, ν (cm^{-1})]: 3296 (N−H), 2843 (aliphatic C−H), 2280 (CN), 660 (SbF_6^-). ^1H NMR (δ (ppm vs Me_4Si)) in CD_2Cl_2: 3.11 (s, 3H), 2.4−2.6 (br, 6H), 2.25 (m, 3H), 2.15 (s, 3H), 2.07 (d, 3H), 1.98 (m, 3H), 1.27 (t, 9H). ESI-TOF/MS data: *m/z* 318 $[M - SbF_6]^+$.

$[Cu(MeCN)(d_{15}$-$Et_3CY)]SbF_6$ (d_{15}-1). Complex d_{15}-**1** (yield 68%) was prepared by the same method as **1** using d_{15}-Et_3CY in place of Et_3CY and was recrystallized from Et_2O/THF to yield colorless crystals. FTIR data [KBr, ν (cm^{-1})]: 3297 (N−H), 2936, 2866 (aliphatic C−H), 2280 (CN), 2228, 2088 (C−D), 658 (SbF_6^-). ^1H NMR (δ (ppm vs Me_4Si)) in CD_2Cl_2: 3.19 (br, 3H), 2.15 (s, 3H), 2.05 (br, 3H), 1.90 (br, 3H). ESI-TOF/MS data: *m/z* 333 $[M - SbF_6]^+$.

$[Cu(MeCN)(iBu_3CY)]SbF_6$ (2). Complex **2** (yield 73%) was prepared by the same method as **1** using iBu_3CY in place of Et_3CY and recrystallized from Et_2O/THF to yield colorless crystals. Anal. Calcd. for $C_{20}H_{42}F_6CuN_4Sb$: C, 37.66; H, 6.63; N, 8.78. Found: C, 37.92; H, 6.69; N, 8.78. FTIR [KBr, ν (cm^{-1})]: 3295 (N−H), 2962 (aliphatic C−H), 2250 (CN), 661 (SbF_6^-). ^1H NMR

(41) Park, G; Lu, F. H.; Ye, N.; Brechbiel, M. W.; Torti, S. V.; Torti, F. M.; Planalp, R. P. *J. Biol. Inorg. Chem.* **1998**, *3*, 449−457.
(42) Varma, K. R.; Caspi, E. *J. Org. Chem.* **1969**, *34*, 2489−2495.
(43) Park, G.; Shao, J.; Lu, F. H.; Rogers, R. D.; Chasteen, N. D.; Brechbiel, M. W.; Planalp, R. P. *Inorg. Chem.* **2001**, *40*, 4167−4175.

(δ (ppm vs Me_4Si)) in CD_2Cl_2: 3.11 (s, 3H), 2.50 (br, 6H), 2.25 (m, 3H), 2.15 (s, 3H), 1.98 (m, 3H), 1.78 (br, 3H), 0.98 (d, 18H). ESI-TOF/MS data: *m*/*z* 402 [M − SbF_6]$^+$.

[Cu(MeCN)(d_6-iBu$_3$CY)]SbF$_6$ (d_6-2). Complex d_6-**2** (yield 73%) was prepared by the same method as **1** using d_6-iBu_3CY in place of Et_3CY and recrystallized from Et_2O/THF to yield colorless crystals. FTIR [KBr, ν (cm^{-1})]: 3295 (N−H), 2963, 2871, 2851 (aliphatic C−H), 2261 (CN), 2202, 2152, 2073 (C−D), 660 (SbF_6^-). ^{1}H NMR (δ (ppm vs Me_4Si)) in CD_2Cl_2: 3.10 (br, 3H), 2.23 (br, 3H), 2.10 (s, 3H), 1.93 (m, 3H), 1.78 (br, 3H), 0.95 (d, 18H). ESI-TOF/MS data: *m*/*z* 408 [M − SbF_6]$^+$.

[Cu(MeCN)(Nd_3-iBu$_3$CY)]SbF$_6$ (Nd_3-2). Complex Nd_3-**2** (yield 66%) was prepared by the same method as **1** using Nd_3-iBu_3CY in place of Et_3CY and recrystallized from Et_2O/THF to yield colorless crystals. FTIR [KBr, ν (cm^{-1})]: 2962, 2873 (aliphatic C−H), 2261 (CN), 660 (SbF_6^-). ^{1}H NMR (δ (ppm vs Me_4Si)) in CD_2Cl_2: 3.06 (br, 3H), 2.50 (br, 6H), 2.20 (br, 3H), 2.08 (s, 3H), 1.93 (m, 3H), 1.80 (br, 3H), 0.94 (d, 18H). ESI-TOF/MS data: *m*/*z* 405 [M − SbF_6]$^+$.

[Cu(MeCN)(Bn$_3$CY)]SbF$_6$ (3). Complex **3** (yield 84%) was prepared by the same method as **1** using Bn_3CY in place of Et_3CY and recrystallized from Et_2O/THF to yield colorless crystals. Anal. Calcd. for $C_{29}H_{36}CuF_6N_4Sb$: C, 47.07; H, 4.90; N, 7.57. Found: C, 47.16; H, 4.92; N, 7.48. FTIR [KBr, ν (cm^{-1})]: 3290 (N−H), 3030 (aromatic C−H), 2844 (aliphatic C−H), 2270 (CN), 1605, 1497 (aromatic ring), 657 (SbF_6^-). ^{1}H NMR (δ (ppm vs Me_4Si)) in CD_2Cl_2: 7.2−7.6 (m, 15H), 3.88 (d, 6H), 3.16 (s, 3H), 2.54 (t, 3H), 2.16 (br, 3H), 1.79 (br, 3H), 1.66 (s, 3H). ESI-TOF/MS data: *m*/*z* 504 [M − SbF_6]$^+$.

[Cu(MeCN)(d_6-Bn$_3$CY)]SbF$_6$ (d_6-3). Complex d_6-**3** (yield 67%) was prepared by the same method as **1** using d_6-Bn_3CY in place of Et_3CY and recrystallized from Et_2O/THF to yield colorless crystals. FTIR [KBr, ν (cm^{-1})]: 3290 (N−H), 3028 (aromatic C−H), 2931, 2877 (aliphatic C−H), 2270 (CN), 2213, 2174, 2079 (C−D), 1606, 1496 (aromatic ring), 658 (SbF_6^-). ^{1}H NMR (δ (ppm vs Me_4Si)) in CD_2Cl_2: 7.33−7.00 (m, 15H), 3.18 (br, 3H), 2.49 (br, 3H), 2.17 (br, 3H), 1.80 (br, 3H), 1.71 (br, 3H). ESI-TOF/MS data: *m*/*z* 510 [M − SbF_6]$^+$.

[Cu(CO)(Et$_3$CY)]SbF$_6$ (4). To a CH_2Cl_2 solution (2 mL) of [Cu(MeCN)$_4$]SbF_6 (122 mg, 2.60×10^{-1} mmol) was added a CH_2Cl_2 solution (2 mL) of Et_3CY (70.4 mg, 3.30×10^{-1} mmol). The reaction solution was stirred for 1 h under CO at 0 °C. Upon addition of Et_2O to the resultant solution, complex **4** precipitated as a white solid. Compound **4** was isolated by filtration (yield 86%) and recrystallized from CH_2Cl_2/Et_2O to yield colorless crystals. Anal. Calcd. for $C_{14}Cl_2H_{29}F_6CuN_3OSb$ (**4**·CH_2Cl_2): C, 26.88; H, 4.67; N, 6.72. Found: C, 26.76; H, 4.73; N, 6.79. FTIR [KBr, ν (cm^{-1})]: 3295 (N−H), 2984, 2940, 2876 (aliphatic C−H), 2055 (CO), 660 (SbF_6^-). ESI-TOF/ MS data: *m*/*z* 317 [M − SbF_6]$^+$.

[Cu(CO)(iBu$_3$CY)]SbF$_6$ (5). Complex **5** (yield 91%) was prepared by the same method as **4** using iBu_3CY in place of Et_3CY and recrystallized from CH_2Cl_2/Et_2O to yield colorless crystals suitable for X-ray structure analysis. Anal. Calcd. for $C_{17}H_{43}F_6CuN_4O_3Sb$ (**5**·2H_2O): C, 34.53; H, 6.56; N, 6.36. Found: C, 34.56; H, 6.29; N, 6.06. FTIR [KBr, ν (cm^{-1})]: 3282 (N−H), 2966, 2877 (aliphatic C−H), 2057 (CO), 660 (SbF_6^-). ESI-TOF/MS data: *m*/*z* 388 [M − SbF_6]$^+$.

[Cu(CO)(Bn$_3$CY)]SbF$_6$ (6). Complex **6** (yield 78%) was prepared by the same method as **4** using iBu_3CY in place of Et_3CY and recrystallized from THF/Et_2O to yield colorless crystals suitable for X-ray structure analysis. Anal. Calcd. for $C_{32}H_{43}CuF_6N_3O_2Sb$ (**6**·Et_2O): C, 47.98; H, 5.19; N, 5.04. Found: C, 47.78; H, 5.19; N, 5.04. FTIR [KBr, ν (cm^{-1})]: 3288 (N−H), 3032 (aromatic C−H), 2867 (aliphatic C−H), 2076 (CO), 1605, 1496 (aromatic ring), 660 (SbF_6^-). ESI-TOF/MS data: *m*/*z* 490 [M − SbF_6]$^+$.

[Cu$_2$(OH)$_2$(Et$_3$CY)$_2$](CF$_3$SO$_3$)$_2$ (10). To a MeOH solution (5 mL) of $Cu(CF_3SO_3)_2$ (38.3 mg, 1.06×10^{-1} mmol) was added a MeOH solution (5 mL) of Et_3CY (22.6 mg, 1.06×10^{-1} mmol), which was stirred for a few minutes. Complex **10** (yield 71%) was isolated as a green powder and recrystallized from Et_2O/MeOH−CH_2Cl_2 to give blue crystals suitable for X-ray structure analysis. Anal. Calcd. For $C_{27}H_{62}Cu_2F_6N_6O_{10}S_2$ (**10**·MeOH·H_2O): C, 34.65; H, 6.68; N, 8.98. Found: C, 34.74; H, 6.49; N, 8.85. FTIR [KBr, ν (cm^{-1})]: 3239 (N−H), 2978 (aliphatic C−H), 1258 ($CF_3SO_3^-$), 1180 ($CF_3SO_3^-$), 640 ($CF_3SO_3^-$). UV−vis (λ_{max}, nm (ϵ, M^{-1} cm^{-1}) in CH_2Cl_2): 347 (2200), 622 (200). ESI-TOF/MS data: *m*/*z* 737 [M − $CF_3SO_3^-$]$^+$.

[Cu$_2$(OH)$_2$(iBu$_3$CY)$_2$](CF$_3$SO$_3$)$_2$ (11). Complex **11** (yield 76%) was prepared by the same method as **10** using iBu_3CY in place of Et_3CY and recrystallized from Et_2O/CH_2Cl_2 to give green crystals suitable for X-ray structure analysis. Anal. Calcd. for $C_{38}H_{82}Cu_2F_6N_6O_9S_2$ (**11**·H_2O): C, 42.56; H, 7.70; N, 7.83. Found: C, 42.26; H, 7.88; N, 7.63. FTIR [KBr, ν (cm^{-1})]: 3249 (N−H), 2958 (aliphatic C−H), 1244 ($CF_3SO_3^-$), 1159 ($CF_3SO_3^-$), 1030 ($CF_3SO_3^-$), 639 ($CF_3SO_3^-$). UV−vis (λ_{max}, nm (ϵ, M^{-1} cm^{-1}) in CH_2Cl_2): 354 (1800), 626 (200). ESI-TOF/MS data: *m*/*z* 905 [M − $CF_3SO_3^-$]$^+$.

[Cu$_2$(OH)$_2$(Bn$_3$CY)$_2$](ClO$_4$)$_2$ (12). To a MeOH solution (5 mL) of $Cu(ClO_4)_2$·$6H_2O$ (68.8 mg, 1.86×10^{-1} mmol) was added a MeOH solution (5 mL) of Bn_3CY (74.0 mg, 1.85×10^{-1} mmol). The reaction solution was stirred for a few minutes, and then complex **12** (yield 67%) was isolated as a green powder and recrystallized from Et_2O/CH_2Cl_2 to give blue crystals suitable for X-ray structure analysis. Anal. Calcd. for $C_{54}H_{74}Cu_2Cl_4N_6O_{14}$ (**12**·4H_2O): C, 52.68; H, 6.22; N, 6.83. Found: C, 52.75; H, 6.03; N, 6.81. FTIR [KBr, ν (cm^{-1})]: 3269, 3244 (N−H), 3062 (aromatic C−H), 2939, 2895 (aliphatic C−H), 1602, 1495 (aromatic ring), 1120 (ClO_4^-). UV−vis (λ_{max}, nm (ϵ, M^{-1} cm^{-1}) in CH_2Cl_2): 359 (2400), 636 (210). ESI-TOF/MS data: *m*/*z* 1059 [M − ClO_4^-]$^+$.

[Cu$_2$(OH)$_2$(Et$_3$CY)$_2$](SbF$_6$)$_2$ (13). A CH_2Cl_2 solution of **1** (5.0 mM, 27.7 mg) was exposed to O_2 at −90 °C and stored for 6 h at −90 °C. After the solution changed from brownish-yellow to blue, the solution was left standing for a few hours at room temperature after which **13** was isolated as blue crystals suitable for X-ray structure analysis (yield 82%). Anal. Calcd. for $C_{24.5}H_{57}ClCu_2F_{12}N_6O_2Sb_2$ (**13**·0.5CH_2Cl_2): C, 26.71; H, 5.21; N, 7.63. Found: C, 26.80; H, 5.05; N, 7.39. FTIR [KBr, ν (cm^{-1})]: 3272 (N−H), 2985, 2942 (aliphatic C−H), 661 (SbF_6^-). ESI-TOF/MS data: *m*/*z* 824 [M − SbF_6^-]$^+$.

Measurements. Electronic absorption spectra were recorded on a JASCO V-570 spectrophotometer. IR spectra of solid compounds were measured as KBr pellets using a JASCO FT/IR-410 spectrophotometer. X-band ESR spectra were obtained using a JEOL RE-1X spectrometer at 77 K. ^{1}H NMR spectral measurements were performed on a Gemini 300 MHz NMR spectrometer in CD_2Cl_2 using TMS as an internal standard. Elemental analysis was carried out on a Perkin-Elmer Japan 2440II CHNO/S that was corrected with acetoanilide. Electrochemical measurements were performed in a glove box using a Bioanalytical Systems (BAS) CV-1B cyclic voltammetry unit, with a three-electrode system consisting of a glassy carbon working electrode, a Pt-wire counter electrode, and an Ag/Ag^+ reference electrode. All measurements were carried out at room temperature with a sweep rate of 50 mV s^{-1} under Ar in degassed and distilled 9:1 (v/v) dichloromethane/acetonitrile, using *n*-Bu_4NClO_4 as a supporting electrolyte. The electrochemical potentials were corrected by measurement of a ferrocene/ferrocenium couple ($E_{1/2}$ = 498 mV, ΔE = 99 mV). Electrospray ionization

Table 1. Crystallographic Data and Experimental Details for Cu(I) Complexes **1**−**3** and **6**

	1	**2**	**3**	**6**
formula	$C_{14}H_{30}CuF_6N_4Sb$	$C_{20}H_{42}CuF_6N_4Sb$	$C_{29}H_{33}CuF_6N_4Sb$	$C_{19}H_{39}CuF_6N_3OP$
fw	553.7	637.86	736.89	1485.75
cryst syst	monoclinic	monoclinic	monoclinic	monoclinic
space group	$P2_1/c$ (No. 14)	$P2_1/n$ (No. 14)	$P2_1/a$ (No. 14)	$P2_1/a$ (No. 14)
a (Å)	10.5097(11)	10.2608(5)	10.515(2)	16.97(3)
b (Å)	13.8322(13)	16.7766(8)	28.900(9)	19.83(2)
c (Å)	15.731(2)	16.3499(10)	10.762(5)	19.62(4)
β (deg)	108.772(5)	110.407(3)	113.402(4)	107.925(17)
V (Å^3)	*2165.2(4)*	*5635.7(58)*	*3001.6(18)*	*6282(19)*
Z	4	4	4	4
ρ_{calcd} (g cm^{-3})	1.698	1.604	1.631	1.571
μ(Mo Kα) (cm^{-1})	22.830	18.828	16.700	16.002
reflns	17075	20160	24334	49757
unique reflns	4971	7170	8562	13829
obsd reflns[a]	2557 ($F_0^2 > 3\sigma(F_0^2)$)	6694 ($F_0^2 > 3\sigma(F_0^2)$)	7260 ($F_0^2 > 3\sigma(F_0^2)$)	26801 ($F_0^2 > 3\sigma(F_0^2)$)
params	307	331	397	805
R1, wR2[a]	0.0313, 0.0450	0.0465, 0.1698	0.0391, 0.1368	0.0701, 0.2128

[a] $R1 = \Sigma||F_0| - |F_c||/\Sigma|F_0|$. $wR2 = [\Sigma(w(F_0^2 - F_c^2)^2)/\Sigma w(F_0^2)^2]^{1/2}$.

Table 2. Crystallographic Data and Experimental Details for Cu(II) Complexes **10**−**13**

	10	**11**	**12**	**13**
formula	$C_{13}H_{28}CuF_3N_3O_4S$	$C_{19}H_{40}CuF_3N_3O_5S$	$C_{28}H_{34}ClCuN_3O_6$	$C_{12}H_{22}CuF_6N_3OSb$
fw	442.98	543.14	607.59	523.61
cryst syst	triclinic	monoclinic	monoclinic	monoclinic
space group	$P\bar{1}$ (No. 2)	$P2_1/c$ (No. 14)	$P2_1/n$ (No. 14)	$P2_1/n$ (No. 14)
a (Å)	9.595(2)	10.183(6)	14.411(7)	9.0475(11)
b (Å)	9.768(2)	12.297(6)	10.865(7)	18.228(2)
c (Å)	12.384(3)	20.33(5)	17.783(9)	11.7273(14)
α (deg)	97.6650(13)			
β (deg)	109.3491(15)	98.29(3)	91.904(6)	100.5340(9)
γ (deg)	113.4832(15)			
V (Å^3)	956.0(3)	2519(7)	2783(3)	1901.5(4)
Z	2	4	4	4
ρ_{calcd} (g cm^{-3})	1.539	1.432	1.450	1.829
μ(Mo Kα) (cm^{-1})	13.016	10.054	9.277	25.964
reflns	7706	19564	20558	20799
unique reflns	4328	5732	6185	4328
obsd reflns[a]	3101 ($F_0^2 > 3\sigma(F_0^2)$)	3116 ($F_0^2 > 3\sigma(F_0^2)$)	18541 ($F_0^2 > 3\sigma(F_0^2)$)	2887 ($F_0^2 > 3\sigma(F_0^2)$)
params	254	323	380	233
R1, wR2[a]	0.0311, 0.0827	0.0762, 0.1826	0.0652, 0.2163	0.0504, 0.1391

[a] $R1 = \Sigma||F_0| - |F_c||/\Sigma|F_0|$. $wR2 = [\Sigma(w(F_0^2 - F_c^2)^2)/\Sigma w(F_0^2)^2]^{1/2}$.

time-of-flight mass spectra (ESI-TOF/MS) were obtained with a Micromass LCT spectrometer. Gas chromatography/mass spectrometry (GC/MS) measurements were carried out on a SHIMADZU GCMS-QP2010. GC was carried out on a SHIMADZU GC-8APF with an FID detector.

Resonance Raman Measurements. A Kr^+ laser (413.1 nm) (Model 2060 Spectra Physics) was employed as the exciting light source. Visible resonance Raman scattering was detected using a liquid nitrogen-cooled CCD detector (Model LN/CCD-1340 × 400PB, Princeton Instruments) attached to a 1 m single polychromator (Model MC-100DG, Ritsu Oyo Kogaku). The slit width and slit height were set to 150 and 10 μm, respectively. The spectral slit width was 3.8 cm^{-1}. The wavenumber per channel was 1.035 cm^{-1}. The laser power used was 36 mW at the sample point. All measurements were carried out with a spinning cell (1000 rpm) kept at −90 °C with a flow of liquid N_2. Raman shifts were calibrated with indene, and the accuracy of the peak positions of the Raman bands was ±1 cm^{-1}.

X-ray Crystallography. Single crystals of **1**−**3** and **6** suitable for X-ray diffraction analyses were obtained from THF or Et_2O/THF solutions after standing for a few days under an Ar atmosphere. Single crystals of **10**−**13** suitable for X-ray diffraction experiments were obtained from Et_2O/MeOH−CH_2Cl_2, Et_2O/CH_2Cl_2, or CH_2Cl_2 solutions after standing for a few days. Each crystal was mounted on a glass fiber, and diffraction data were collected on a Rigaku/MSC Mercury CCD using graphite monochromated Mo Kα radiation at −100 °C. Crystal data and experimental details are listed in Tables 1 and 2.

All eight structures were solved by a combination of direct methods (SIR 92 and SHELEXS 97) and Fourier techniques. All non-hydrogen atoms were refined anisotropically. Hydrogen atoms were refined using the riding model. A Sheldrick weighting scheme was employed. Plots of $\Sigma w(|F_0| - |F_c|)^2$ versus $|F_0|$, reflection order in data collection, sin θ/λ, and various classes of indices showed no unusual trends. Neutral atomic scattering factors were obtained from Cromer and Waber.[44] Anomalous dispersion terms were included in F_{calc}[45], and the values for $\Delta f'$ and $\Delta f''$ were those of Creagh and McAuley.[46] The values for the mass attenuation

(44) Cromer, D. T.; Waber, J. T. *International Tables for X-ray Crystallography*; Kynoch Press: Birmingham, UK, 1974; Vol. 4.
(45) Ibers, J. A.; Hamilton, W. C. *Acta Crystallogr.* **1964**, *17*, 781.
(46) Creagh, D. C.; McAuley, W. J. *International Tables for X-ray Crystallography*; Kluwer: Boston, 1992; Vol. C, Table 4.2.6.8, pp 219−222.

coefficients are those of Creagh and Hubbell.[47] All calculations were performed using the crystallographic software package, CrystalStructure.[48,49] A packing diagram of the unit cell and a complete set of crystallographic tables including positional parameters, anisotropic thermal factors, and bond lengths and angles are included in the Supporting Information.

Thermal Decomposition Kinetics. The thermal decomposition reactions of the bis(μ-oxo)dicopper(III) species were characterized by monitoring the decrease in the absorption intensity at 410 nm in a 1 mm path length quartz cell, whose temperature was controlled by an Oxford thermostat (experimental error was $\pm$0.1 °C). The data were analyzed with Delta Graph (Polaroid Computing) running on a Macintosh computer and fitted to an exponential function by the nonlinear least-squares method.

Analysis of Decomposition Products of Bis(μ-oxo)dicopper(III) Complexes 7−9 by GC and GC/MS. The bis(μ-oxo)-dicopper(III) complexes, **7**−**9**, were prepared by bubbling excess O_2 into THF (0.5 mM, 3 mL) solutions of **1**−**3** treated with 5 cycles of vacuum/purging with Ar gas at 165 K. The solutions were then stored at −80 °C for 2 h. The addition of 5 mL of *n*-hexane produced precipitates of the copper(II) complexes. After filtration, the decomposition products were monitored by GC and GC/MS.

Analysis of the Products of the Decomposition Reaction of Bis(μ-oxo)dicopper(III) Complex 7 Monitored by ^{1}H NMR. The dicopper(III) complex $[Cu_2(\mu\text{-}O)_2(Et_3CY)_2](SbF_6)_2$ (**7**) was prepared by the addition of excess O_2 to a CH_2Cl_2 (2 mL) solution of **1** (2 mM, 2.2 mg) at 183 K. The CH_2Cl_2 solution was treated with 5 cycles of vacuum/purging with Ar gas before use. After the resulting solution was stored at −80 °C for 2 h to complete the decomposition reaction, it was warmed to room temperature. The solvent was removed under reduced pressure to yield a blue powder. To a $CHCl_3$ (3 mL) solution of the powder was added 3 mL of concentrated aqueous ammonia with stirring for 30 min. The solution was separated into two layers, and the organic compound was extracted with $CHCl_3$ (5 × 3 mL) and dried with Na_2SO_4. The solvent was removed by evaporation under reduced pressure to yield a colorless oil (yield: 81%), which was characterized by ^{1}H NMR.

GC Conditions. Column PEG-20M Chromosorb WAW DMCS; column length 3 m; column temperature 95 °C (heating to 150 °C with 6 °C/min after 2.5 min); 200 kPa; hydrogen pressure 70 kPa; and internal standard material 1,2,4-trichlorobenzene.

C_6H_5CHO. t_R 2.05 min.

GC/MS Conditions. Column DB-5 ms; column length 30.0 m; column temperature 50 °C (heating to 80 °C with 3 °C/min after 1 min and then heating to 180 °C with 20 °C/min); injection temperature 200 °C; 80 kPa; and internal standard material 1,2,4-trichlorobenzene.

2-Hydroxytetrahydrofuran. t_R 3.38 min, *m*/*z* 87 (M^+, using $^{16}O_2$), 89 (M^+, using $^{18}O_2$).

γ-Butyrolactone. t_R 6.36 min, *m*/*z* 86 (M^+, using $^{16}O_2$), 88 (M^+, using $^{18}O_2$).

C_6H_5CHO. t_R 6.72 min, *m*/*z* 106 (M^+, using $^{16}O_2$), 108 (M^+, using $^{18}O_2$).

Results and Discussion

Synthesis and Characterization of Cu(I) Complexes 1−6. The ligands with rigid cyclohexane frames, R_3CY (R = Et, iBu, and Bn), were prepared according to the previously published methods[40,43] and were used in synthesis of the Cu(I) complexes.

The Cu(I) complexes $[Cu(MeCN)(R_3CY)]SbF_6$ (R = Et (**1**), iBu (**2**), and Bn (**3**)) and $[Cu(CO)(R_3CY)]SbF_6$ (R = Et (**4**), iBu (**5**), and Bn (**6**)) were synthesized from R_3CY and $[Cu(MeCN)_4]SbF_6$ under anaerobic conditions in THF or CH_2Cl_2. These Cu(I) complexes are very air-sensitive, and the solutions of **1**−**6** are immediately oxidized to Cu(II) complexes under air at room temperature.

Complexes **1**−**3** were recrystallized from THF/Et_2O under Ar and characterized by elemental and X-ray structure analyses, ^{1}H NMR spectroscopy, FTIR spectroscopy, ESI mass spectrometry, and cyclic voltammetry. Coordination of an MeCN to the copper(I) ions in the solution was confirmed by observation of a broad peak of methyl protons at ~2.2 ppm in CD_2Cl_2 in the ^{1}H NMR spectra and a weak ν(C≡N) band at ~2300 cm^{-1} in the FTIR spectra. Three crystal structures of **1**−**3** have been determined by X-ray structure analysis. The crystal parameters and experimental details are summarized in Table 1. Molecular structures and the selected bond lengths and angles for **1**−**3** are given in Figure 1 and Table 3, respectively. For **3**, disorder is noted for a benzyl methylene carbon (C(21)/C(22)) and secondary amine nitrogen atoms (N(3)/N(4)). Each cation of **1**−**3** has a tetrahedral geometry with three secondary amine nitrogen atoms of R_3CY and the MeCN ligand. The average Cu−N_{CY} bonds for **1**−**3** may be influenced by the bulkiness of the substituent groups **1** {2.108(4) Å} < **2** {2.120(2) Å} < **3** {2.1318(4) Å}. The average Cu−N_{CY} bond lengths for **1** and **2** are shorter than those of the copper(I) complexes of macrocyclic ligands with two or three five-membered chelate rings. These examples include iPr_3TACN {1,4,7-triisopropyl-1,4,7-triazacyclononane: Cu−N = 2.1370(3) Å} or iPr_3-TACD {1,4,7-triisopropyl-1,4,7-triazacyclodecane: Cu−N = 2.1277(6) Å}.[50] This trend indicates that the electron donor characteristics of Et_3CY and iBu_3CY to the copper(I) ion are stronger than those of iPr_3TACN and iPr_3TACD. The relationship between structures and oxygenation reactivities of copper(I) complexes was previously investigated using copper complexes with iPr_3TACN, iPr_3TACD, and iPr_3-TACDD (1,5,9-triisopropyl-1,5,9-triazaacyclododecane) and discussed by Lam et al.[50] as follows: the copper−oxygen reactivity is drastically affected by the magnitude of the deviations of the Cu ion from the mean planes defined by the three N-donor atoms (the N_3 plane) and the three iPr methine carbon atoms (the $(CH)_3$ plane) for the macrocyclic ligands. Copper complexes with larger deviations exhibit higher oxygenation reactivity relative to copper complexes with smaller deviations. The deviations of the Cu(I) ions from

(47) Creagh, D. C.; Hubbell, J. H. *International Tables for Crystallography*; Kluwer: Boston, 1992; Vol. C, Table 4.2.4.3, pp 200−206.
(48) *CrystalStructure 3.7.0: Crystal Structure Analysis Package*; Rigaku and Rigaku/MSC (2000−2005): The Woodlands, TX.
(49) Watkin, D. J.; Prout, C. K. C.; Carruthers, J. R.; Betteridge, P. W. *CRYSTALS Issue 10*; Chemical Crystallography Laboratory: Oxford, 1996.
(50) Lam, B. M.; Halfen, J. A.; Young, V. G., Jr.; Hagadorn, J. R.; Holland, P. L.; Lledós, A.; Cucurull-Sánchez, L.; Novoa, J. J.; Alvarez, S.; Tolman, W. B. *Inorg. Chem.* **2000**, *39*, 4059−4072.

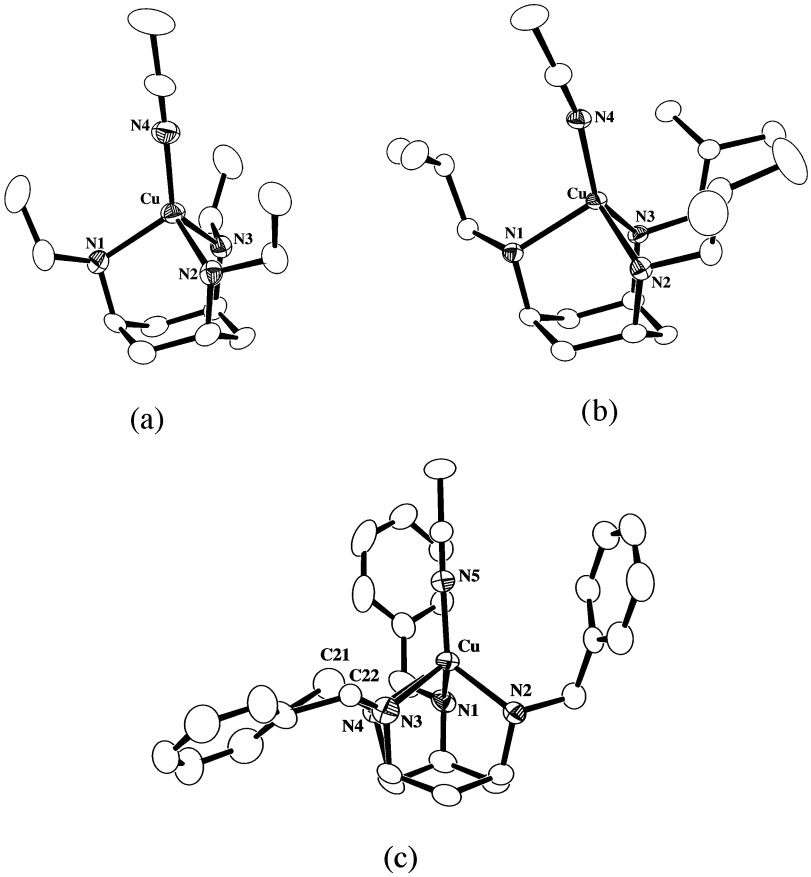

Figure 1. ORTEP views of the cationic portions of Cu(I) complexes **1** (a), **2** (b), and **3** (c) with the atom numbering scheme (50% probability ellipsoids).

Table 3. Selected Bond Lengths (Å) and Angles (deg) for **1**−**3**

1		**2**		**3**	
Cu−N(1)	2.087(4)	Cu−N(1)	2.141(2)	Cu−N(1)	2.106(2)
Cu−N(2)	2.109(4)	Cu−N(2)	2.081(2)	Cu−N(2)	2.1050(17)
Cu−N(3)	2.128(5)	Cu−N(3)	2.138(2)	Cu−N(3)	2.169(6)
Cu−N(4)	1.881(5)	Cu−N(4)	1.900(2)	Cu−N(4)	2.147(4)
N(1)−Cu−N(2)	95.2(2)	N(1)−Cu−N(2)	94.21(6)	Cu−N(5)	1.880(2)
N(1)−Cu−N(3)	93.1(2)	N(1) Cu−N(3)	94.86(6)	N(1)−Cu−N(2)	96.08(8)
N(1)−Cu−N(4)	128.6(2)	N(1)−Cu−N(4)	114.35(7)	N(1)−Cu−N(3)	102.44(16)
N(2)−Cu−N(3)	97.0(2)	N(2)−Cu−N(3)	95.59(6)	N(1)−Cu−N(4)	87.66(14)
N(2)−Cu−N(4)	120.0(2)	N(2)−Cu−N(4)	138.18(7)	N(1)−Cu−N(5)	123.20(9)
N(3)−Cu−N(4)	115.9(2)	N(3)−Cu−N(4)	110.77(7)	N(2)−Cu−N(3)	88.13(13)
				N(2)−Cu−N(4)	99.31(11)
				N(2)−Cu−N(5)	124.68(7)
				N(3)−Cu−N(4)	17.64(17)
				N(3)−Cu−N(5)	115.18(17)
				N(4)−Cu−N(5)	117.72(14)

the N_3 plane and from the plane defined by the three secondary methylene carbon atoms (the $(CH_2)_3$ plane) in the *N*-alkyl substituent groups of **1**−**3** are 1.1046/0.3869, 1.1161/0.3448, and 1.1187/0.4108 Å, respectively (Figure 2 and Table 4). For **1**−**3**, the distances of the Cu(I) ion from the N_3 plane (Cu···N_3) are shorter than those of [Cu(MeCN)-(iPr_3TACN)]$^+$ and [Cu(MeCN)(iPr_3TACD)]$^+$, and the distances between the $(CH_2)_3$ plane and the N_3 plane, ((CH_2)$_3$···N_3) are shorter than those between the N_3 and $(CH)_3$ planes ((CH)$_3$···N_3) in the Cu(I) complexes of iPr_3TACN and iPr_3-TACD. The deviations of the Cu(I) ion from the $(CH_2)_3$ planes that are determined from the distance between Cu···N_3 and $(CH_2)_3$···N_3 in **1**−**3** are larger than the deviations of the Cu(I) ion from the $(CH)_3$ planes that are obtained from the distance between Cu···N_3 and $(CH)_3$···N_3 in the Cu(I) complexes of iPr_3TACN and iPr_3TACD. Thus, the reactivites

Table 4. Deviations of Cu Ions from Plane Defined by Three Amine Nitrogen Atoms and from Plane Defined by Three Methylene or Methine Carbons (Å)

complex	Cu···N_3	$(CH_2)_3$···N_3 $(CH)_3$···N_3	Cu···$(CH_2)_3$ Cu···$(CH)_3$
1	1.1046(6)	0.3869(6)	0.7177(6)
2	1.1161(3)	0.3448(3)	0.7713(3)
3	1.1187(17)	0.4108(17)	0.7079(17)
10	1.1812(4)	0.4069(4)	0.7743(4)
11	1.1711(10)	0.3948(10)	0.7763(10)
12	1.1768(2)	0.4794(2)	0.6974(2)
[Cu(MeCN)(iPr_3TACN)]$^{+a}$	1.40	0.70	0.70
[Cu(MeCN)(iPr_3TACD)]$^{+a}$	1.26	1.28	−0.02

[a] Ref 50.

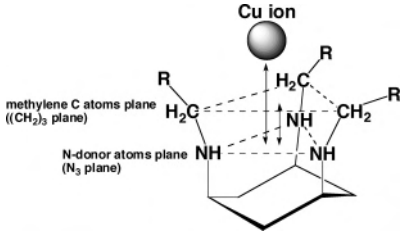

Figure 2. Deviations of Cu(I) ions from the plane (N_3 plane) defined by three amine nitrogens and from the plane ($(CH_2)_3$ plane) defined by three methylene carbons (Å).

Table 5. Electrochemical Data for Cu(I) Complexes[a]

complex	E_{pa}	E_{pc}	ΔE_p	$E_{1/2}$
1	398	289	109	344
2	450	337	113	394
3	398	293	105	346

[a] All potentials are reported vs SCE in 9:1 (v/v) CH_2Cl_2/MeCN at room temperature. The concentration of the supporting electrolyte TBAP is 0.1 M. The concentration of the complex is 1 mM. Scan rate $v = 50$ mV s^{-1}.

of **1**−**3** with O_2 were expected to be higher than the reactivities of the Cu(I) complexes with iPr_3TACN and iPr_3-TACD.

The redox potentials of **1**−**3** were obtained by cyclic voltammetry (CV) measurements. The results are shown in Table 5 and Figure S1. The redox profiles measured in 9:1 (v/v) CH_2Cl_2/MeCN showed quasi-reversible waves, and the $E_{1/2}$ values (vs SCE) of **1**−**3** were 344, 394, and 346 mV, respectively. The $E_{1/2}$ values of **1**−**3** were significantly lower relative to those of $[Cu(MeCN)(iPr_3TACD)]^+$ (600 mV vs SCE), $[Cu(MeCN)(Me_3TACD)]^+$ (400 mV vs SCE), and $[Cu(MeCN)(Bn_3TACD)]^+$ (440 mV vs SCE).[50] These findings suggest that the electron donor capabilities of the R_3-CY compounds are greater than those of triazamacrocyclic ligands and that the R_3CY ligands are more effective at stabilizing higher oxidation states than R_3TACN and R_3-TACD.

Carbonyl adducts of $[Cu(CO)(R_3CY)]SbF_6$ (where R = Et (**4**), iBu (**5**), and Bn (**6**)) were also prepared as Cu(I) complexes and recrystallized from CH_2Cl_2/Et_2O or THF/Et_2O under CO gas. Fortunately, we obtained a single crystal of **6** suitable for X-ray structure analysis. Crystal data and relevant experimental details are summarized in Table 1. The ORTEP view and the selected bond lengths and angles for **6** are shown in Figure 3 and Table 6, respectively. The crystal of **6** included two independent molecules, **6a** and **6b**, in the unit cell. The Cu(I) ion of **6a** is surrounded by three benzyl groups, while that of **6b** is surrounded by two benzyl groups with the third benzyl group extending away from the metal ion. Both **6a** and **6b** have tetrahedral coordination structures with a single carbon monoxide ligand and three amine nitrogens. The Cu−C and C≡O bond lengths for **6a** and **6b** are 1.813(5)/1.129(7) and 1.777(6)/1.152(7) Å, respectively. In general, the C≡O stretching frequency of a carbonyl complex strongly correlates with the electronic properties of the metal center. A stronger electron donating ligand lowers the frequency because the π-back-donation from the metal center to the carbonyl group weakens the C≡O bond.[51−53] The C≡O stretching vibrations ν(CO) for **4**−**6**, as measured by FTIR spectroscopy, have absorption peaks at 2055, 2057, and 2076 cm^{-1}, respectively, indicating that the electron density on the copper center increases according to the following order: $Bn_3CY < iBu_3CY < Et_3CY$. The ν(CO) values of Cu(I) carbonyl complexes with iPr_3TACN, Bn_3TACN, Me_3TACD, iPr_3TACD, and Bn_3TACD are 2067, 2084, 2086, 2063, and 2074 cm^{-1}, respectively.[19,50] These findings indicate that the electron donor capabilities of the R_3CY compounds are greater than those of the triazamacrocyclic ligands, except for compounds with benzyl groups.

Synthesis and Characterization of Cu(II) Complexes 10−12. There are very few reports of characterization of bis-μ-hydroxo dicopper(II) complexes, which are obtained from the reaction of capped-type ligand Cu(I) complexes with dioxygen. Thus, investigations of dicopper(II) complexes with R_3CY (where R = Et (**10**), iBu (**11**), and Bn (**12**)) may be important from the viewpoint of understanding structure−reactivity relationships of the intermediates generated in reactions of Cu(I) complexes and dioxygen. The Cu(II) complexes investigated are of the type $[Cu_2(OH)_2(R_3CY)_2](X)_2$ (where for **10**, R = Et and $X^- = CF_3SO_3^-$; for **11**, R = iBu and $X^- = CF_3SO_3^-$; and for **12**, R = Bn and $X^- = ClO_4^-$). These complexes were synthesized in reactions of R_3CY with $Cu(X)_2$ (where $X = CF_3SO_3^-$ or ClO_4^-) in MeOH by the synthetic method described in the Experimental Procedures. Complexes **10**−**12** were characterized on the basis of elemental analysis, X-ray structure analyses, ESI mass spectrometry, and UV−vis spectroscopy.

The UV−vis spectra of **10**−**12** showed LMCT bands originating from OH^- to Cu(II) at around 347−359 nm in CH_2Cl_2 solutions and d−d transition bands with a shoulder peak in the lower energy region at 622 nm ($\epsilon = 200$ M^{-1} cm^{-1}) for **10**, 626 nm ($\epsilon = 200$ M^{-1} cm^{-1}) for **11**, and 636 nm ($\epsilon = 210$ M^{-1} cm^{-1}) for **12**. These spectra indicate that complexes **10**−**12** have square pyramidal geometries.[54]

The crystal structures of complexes **10**−**12** were determined, and the crystal parameters are summarized in Table 2, which also includes experimental details. The ORTEP views are shown in Figure 4. The selected bond lengths and angles are listed in Table 7. Unlike complexes **10** and **11**, complex **12** formed a molecular structure with six benzyl groups spreading out from the $Cu_2(OH)_2$ center in apparent avoidance of steric repulsions. τ values vary from 0, for an idealized square pyramid, to 1, for an idealized trigonal bipyramid.[55] The τ values of the coordination geometries around the Cu(II) ions were 0.12, 0.05, and 0.00 for complexes **10**−**12**, respectively. This indicates that com-

(51) Kitajima, N.; Fujisawa, K.; Fujimoto, C.; Moro-oka, Y.; Hashimoto, S.; Kitagawa, T.; Toriumi, K.; Tatsumi, K.; Nakamura, A. *J. Am. Chem. Soc.* **1992**, *114*, 1277−1291.
(52) Imai, S.; Fujisawa, K.; Kobayashi, T.; Shirasawa, N.; Fujii, H.; Yoshimura, T.; Kitajima, N.; Moro-oka, Y. *Inorg. Chem.* **1998**, *37*, 3066−3070.
(53) Fujisawa, K.; Ono, T.; Ishikawa, Y.; Amir, N.; Miyashita, Y.; Okamoto, K.; Lehnert, N. *Inorg. Chem.* **2006**, *45*, 1698−1713.
(54) Karlin, K. D.; Hayes, J. C.; Juen, S.; Hutchinson, J. P.; Zubieta, J. *Inorg. Chem.* **1982**, *21*, 4106−4108.
(55) Addison, A. W.; Rao, T. N.; Reedijk, J.; van Rijn, J.; Verschoor, G. C. *J. Chem. Soc., Dalton Trans.* **1984**, 1349−1356.

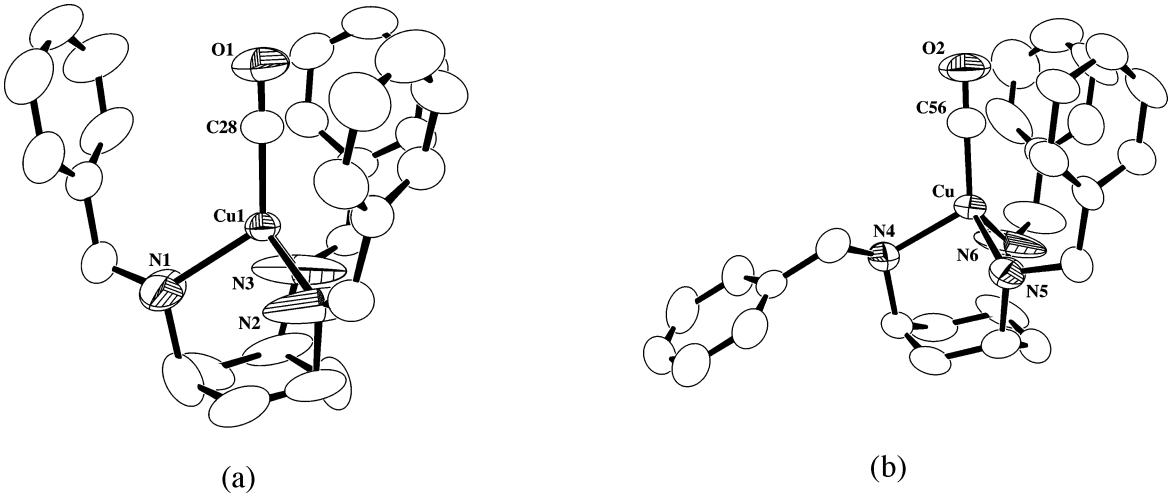

Figure 3. ORTEP views of the cationic portions of the Cu(I) complexes **6a** (a) and **6b** (b) with the atom numbering scheme (50% probability ellipsoids).

Table 6. Selected Bond Lengths (Å) and Angles (deg) for **6a** and **6b**

6a		**6b**	
Cu(1)−C(28)	1.813(5)	Cu(2)−C(56)	1.777(6)
C(28)−O(1)	1.129(7)	C(56)−O(2)	1.152(7)
Cu(1)−N(1)	2.023(7)	Cu(2)−N(4)	2.120(4)
Cu(1)−N(2)	2.038(8)	Cu(2)−N(5)	2.036(5)
Cu(1)−N(3)	2.114(7)	Cu(2)−N(6)	2.024(7)
N(1)−Cu(1)−N(2)	92.6(3)	N(4)−Cu(2)−N(5)	93.00(18)
N(1)−Cu(1)−N(3)	91.8(3)	N(4)−Cu(2)−N(6)	95.5(2)
N(1)−Cu(1)−C(28)	121.4(2)	N(4)−Cu(2)−C(56)	117.9(2)
N(2)−Cu(1)−N(3)	94.9(3)	N(5)−Cu(2)−N(6)	96.3(2)
N(2)−Cu(1)−C(28)	126.7(2)	N(5)−Cu(2)−C(56)	124.8(2)
N(3)−Cu(1)−C(28)	120.7(2)	N(6)−Cu(2)−C(56)	122.1(2)

plexes **10**−**12** have slightly distorted square pyramidal coordination structures. The Cu···Cu separation distances for complexes **10**−**12** are 3.0180(4), 3.0673(12), and 2.9957(2), respectively. The deviations of Cu(II) ion from the N_3 plane, the distances between N_3 and $(CH_2)_3$ planes, and deviations of Cu(II) ion from the $(CH_2)_3$ plane for **10**−**12** were 1.1812/0.4069/0.7743, 1.1711/0.3948/0.7763, and 1.1768/0.4794/0.6974 Å, respectively (Table 4). These results indicate that the Cu(II) ion of each of the complexes **10**−**12** is located out of the $(CH_2)_3$ plane, making it accessible to solvent and substrate molecules. The ligands R_3CY have three N−H protons that induce attractive noncovalent interactions such as hydrogen bonding and electrostatic interactions. The N_{eq}···O(H) interatomic distances for complexes **10**−**12** were 2.866(2)/2.907(2), 2.849(7)/2.903(7), and 2.8554(15)/2.8725(13), respectively, and the N−H···O(H) angles were 88.34(16)/92.8(2), 89.7(5)/90.7(4), and 91.84(10)/91.99(9), respectively. Thus, the interaction between the two N−H protons of R_3CY and hydroxo anions is an electrostatic interaction. As described next, this electrostatic interaction is expected to affect to the character of the bis(μ-oxo)dicopper(III) species whose structure should be similar to the bis(μ-hydroxo)dicopper(II) species.

Reaction of Cu(I) Complexes 1−3 with Dioxygen. Upon exposure of the THF solutions of complexes **1**−**3** to dioxygen at −108 °C, the solution immediately turns yellow. The products were characterized as bis(μ-oxo)dicopper(III) complexes **7**−**9** (Scheme 1) on the basis of UV−vis spectra that show two bands characteristic of bis(μ-oxo)dicopper(III) species at 304 nm (ϵ = 15 000 M^{-1} cm^{-1})/411 nm (ϵ = 19 000 M^{-1} cm^{-1}) for **7**, 316 nm (ϵ = 14 000 M^{-1} cm^{-1})/419 nm (ϵ = 19 000 M^{-1} cm^{-1}) for **8**, and 306 nm (ϵ = 4600 M^{-1} cm^{-1})/413 nm (ϵ = 4900 M^{-1} cm^{-1}) for **9** (Table 8). The solution of **9** immediately changed from brownish-yellow to blue even at −108 °C. The ϵ values of **9** were much lower than those of **7** and **8** because of the immediate decomposition of **9**.

To study the effect of substituent groups on reactivity of the complexes with dioxygen, deuterated complexes corresponding to complexes **1**−**3** were synthesized d_{15}-**1** (ethyl-deuterated), d_6-**2** (isobutyl methylene-deuterated), and d_6-**3** (benzyl methylene-deuterated). These deuterated complexes gave complexes d_{15}-**7**, d_6-**8**, and d_6-**9** with greater thermal stability than complexes **7**−**9** obtained under the same conditions. The rate constants (k_{dec}) and half-lives ($\tau_{1/2}$) are shown in Table 9. Absorption bands are found at 310 nm (ϵ = 15 000 M^{-1} cm^{-1})/411 nm (ϵ = 20 000 M^{-1} cm^{-1}) for d_{15}-**7**, 318 nm (ϵ = 17 000 M^{-1} cm^{-1})/415 nm (ϵ = 20 000 M^{-1} cm^{-1}) for d_6-**8**, and 308 nm (ϵ = 17 000 M^{-1} cm^{-1})/415 nm (ϵ = 23 000 M^{-1} cm^{-1}) for d_6-**9**, respectively. Resonance Raman spectral measurements for **7**−**9** were obtained in a range including the ν(Cu−O) stretching vibration. Fortunately, the ν(Cu−O) stretching vibration for d_6-**9** was obtained, although that of **9** was not detected because of its instability. The bands assignable to the ν(Cu−O) stretching vibration measured using $^{16}O_2$ and $^{18}O_2$ were observed at 553, 581/547 cm^{-1} for **7**, 571/546 cm^{-1} for **8**, and 585/560 cm^{-1} for d_6-**9**, respectively. Furthermore, each of the complexes is ESR silent. These observations indicate that complexes **7**−**9** are bis(μ-oxo)dicopper(III) complexes.[9,10,12,14,19,20,22]

Absorption spectra of complexes **7**−**9** exhibit two bands between 306 and 317 nm and 406−413 nm that are assignable to the $\pi_\sigma^* \rightarrow d_{xy}$ and $\sigma^* \rightarrow d_{xy}$ charge-transfer bands originating from the oxide to the Cu(III) in the bis(μ-oxo) complex.[56] Stack et al. reported that the latter CT band shifts to a lower energy region in a manner dependent

(56) Henson, M. J.; Mukherjee, P.; Root, D. E.; Stack, T. D. P.; Solomon, E. I. *J. Am. Chem. Soc.* **1999**, *121*, 10332−10345.

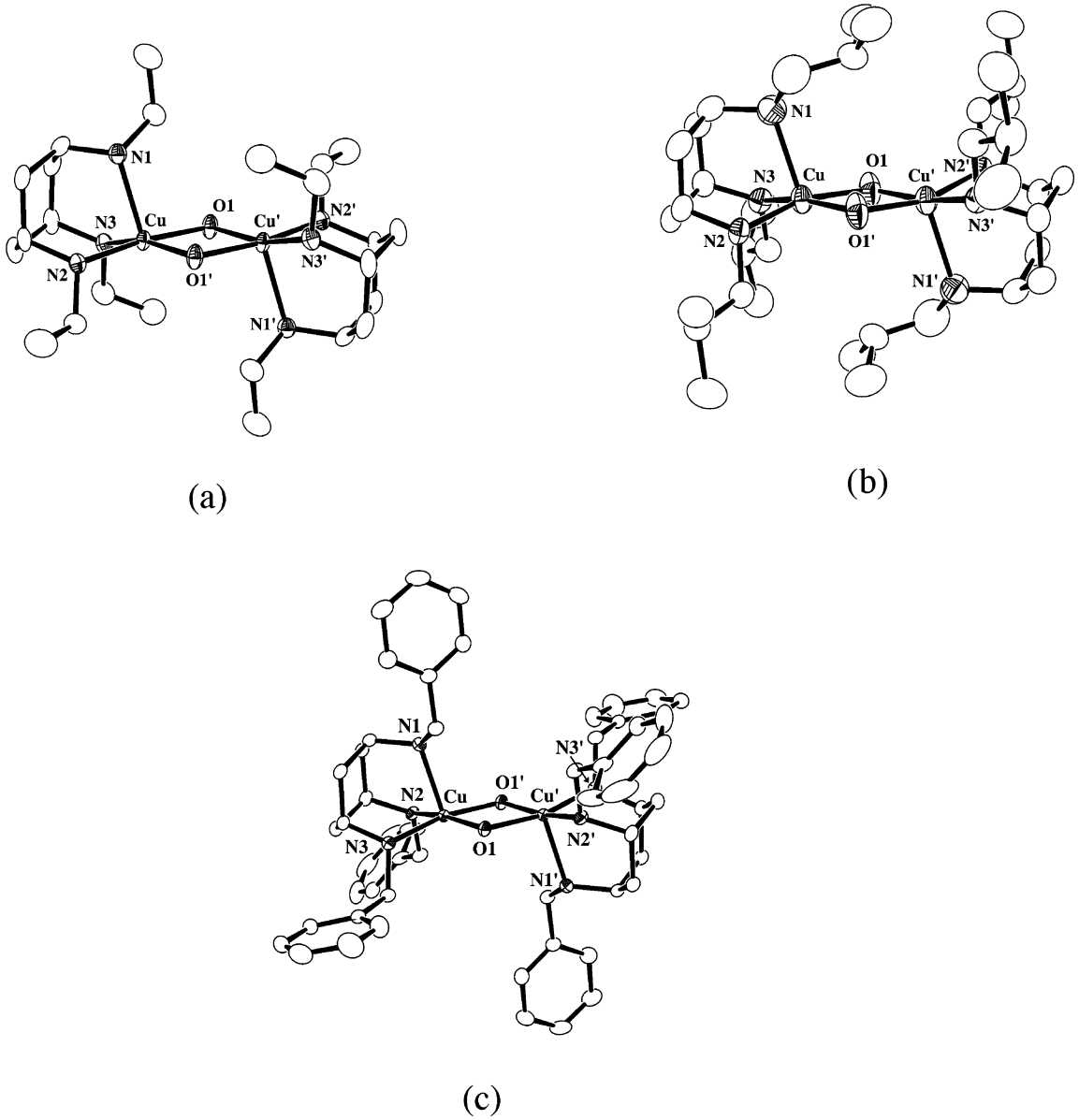

Figure 4. ORTEP views of the cationic portions of the Cu(II) complexes **10** (a), **11** (b), and **12** (c) with the atom numbering scheme (50% probability ellipsoids).

upon an increase in the steric bulk of the ligands.[14] The CT bands measured for complexes **7** and **8** exhibit the same tendency. The Cu−O stretching vibration bands for complexes **7**−**9** were observed in lower energy regions than those of bis(μ-oxo)dicopper complexes with R_3TACN (R = iPr, Bn, and Me) and R_3TACD (Me and Bn). These results suggest that the N-donor characteristics of R_3CY ligands are stronger than those of R_3TACN and R_3TACD.

Activation of Dioxygen by Cu(I) Complexes 1−3 and Decomposition Reaction of the Bis(μ-oxo)dicopper(III) Complexes 7−9. We previously reported that **2** reacts with oxygen in CH_2Cl_2 at 300 K at the β-methine carbon of isobutyl group of the ligand iBu_3CY that has a higher C−H bond energy than the C−H bond energy of amino and benzyl groups.[40] It is interesting that the copper complex with iBu_3-CY has a relatively high oxygenation potential for hydrocarbons using dioxygen. In this work, we carried out a detailed investigation on an intramolecular oxygenation reaction using bis(μ-oxo)dicopper(III) species with Bn_3CY, iBu_3CY, and Et_3CY ligands that have benzyl groups with weak methylene C−H bonds, isobutyl groups with intermediate C−H bonds, and ethyl groups with strong C−H bonds.

Each of the decomposition rates of complexes **7**−**9** obeyed first-order kinetics. The $\tau_{1/2}$ values of complexes **7**−**9** in THF at −90 °C were 2490, 860, and 18 s, respectively (Table 9). The thermal stability of complexes **7**−**9** decreased according to the increase in the size of the *N*-alkyl substituents, Et > iBu > Bn. This tendency is in agreement with the results reported by Stack et al.; bis(μ-oxo)dicopper(III) complexes $[Cu_2(\mu\text{-}O)_2(CD^{R,R'})_2]^{2+}$ {$CD^{R,R'}$ = (1R,2R)-cyclohexanediamine, (R,R′) = (Me,Me), (Me,Et), and (Et,Et)}, in which the hydrogen atom of the NC^{α}−H site on alkyl substituents is abstracted more easily, showed lower stability.[20] The benzyl hydrogen atom of the Bn_3CY ligand was easily abstracted relative to the methylene hydrogen atoms of the α-carbons of Et_3CY and iBu_3CY. The H atoms of the

Table 7. Selected Bond Lengths (Å), Angles (deg), and Interatomic Distances (Å) for **10**−**13**

	10				**11**		
Cu−N(1)	2.282(2)	Cu−N(2)	2.0544(17)	Cu−N(1)	2.298(6)	Cu−N(2)	2.031(5)
Cu−N(3)	2.018(2)	Cu−O(1)	1.944(2)	Cu−N(3)	2.038(6)	Cu−O(1)	1.970(5)
Cu−O(1′)	1.9464(13)	Cu···Cu′	3.0180(4)	Cu−O(1′)	1.990(4)	Cu···Cu′	3.0673(12)
N(1)−Cu−N(2)	86.04(9)	N(1)−Cu−N(3)	93.70(10)	N(1)−Cu−N(2)	92.4(2)	N(1)−Cu−N(3)	87.9(2)
N(1)−Cu−O(1)	103.37(10)	N(1)−Cu−O(1′)	99.35(8)	N(1)−Cu−O(1)	104.1(2)	N(1)−Cu−O(1′)	102.7(2)
N(2)−Cu−N(3)	94.62(9)	N(2)−Cu−O(1)	91.52(8)	N(2)−Cu−N(3)	95.7(2)	N(2)−Cu−O(1)	90.8(2)
N(2)−Cu−O(1′)	169.27(9)	N(3)−Cu−O(1)	162.21(10)	N(2)−Cu−O(1′)	163.2(2)	N(3)−Cu−O(1)	166.1(2)
N(3)−Cu−O(1′)	94.27(8)	O(1)−Cu−O(1′)	78.25(7)	N(3)−Cu−O(1′)	92.2(2)	O(1)−Cu−O(1′)	78.5(2)
Cu−O(1)−Cu′	101.75(9)			Cu−O(1) −Cu′	101.5(2)		
	12				**13**		
Cu−N(1)	2.2495(11)	Cu−N(2)	2.0301(10)	Cu−N(1)	2.81(6)	Cu−N(2)	2.031(4)
Cu−N(3)	2.0451(11)	Cu−O(1)	1.9708(9)	Cu−N(3)	2.044(5)	Cu−O	1.946(4)
Cu−O(1′)	1.9770(9)	Cu···Cu′	2.9957(2)	Cu−O′	1.941(4)	Cu···Cu′	3.0495(9)
N(1)−Cu−N(2)	89.04(4)	N(1)−Cu−N(3)	91.11(4)	N(1)−Cu−N(2)	88.4(2)	N(1)−Cu−N(3)	90.0(2)
N(1)−Cu−O(1)	102.49(4)	N(1)−Cu−O(1′)	99.92(4)	N(1)−Cu−O	104.2(2)	N(1)−Cu−O′	106.0(2)
N(2)−Cu−N(3)	94.53(4)	N(2)−Cu−O(1)	167.29(4)	N(2)−Cu−N(3)	96.1(2)	N(2)−Cu−O	164.9(2)
N(2)−Cu−O(1′)	91.58(4)	N(3)−Cu−O(1)	90.62(4)	N(2)−Cu−O′	92.19(19)	N(3)−Cu−O	92.4(2)
N(3)−Cu−O(1′)	167.48(4)	O(1)−Cu−O(1′)	81.28(3)	N(3)−Cu−O′	162.39(19)	O−Cu−O′	76.63(19)
Cu−O(1)−Cu′	98.72(4)			Cu−O−Cu′	103.4(2)		

Scheme 1

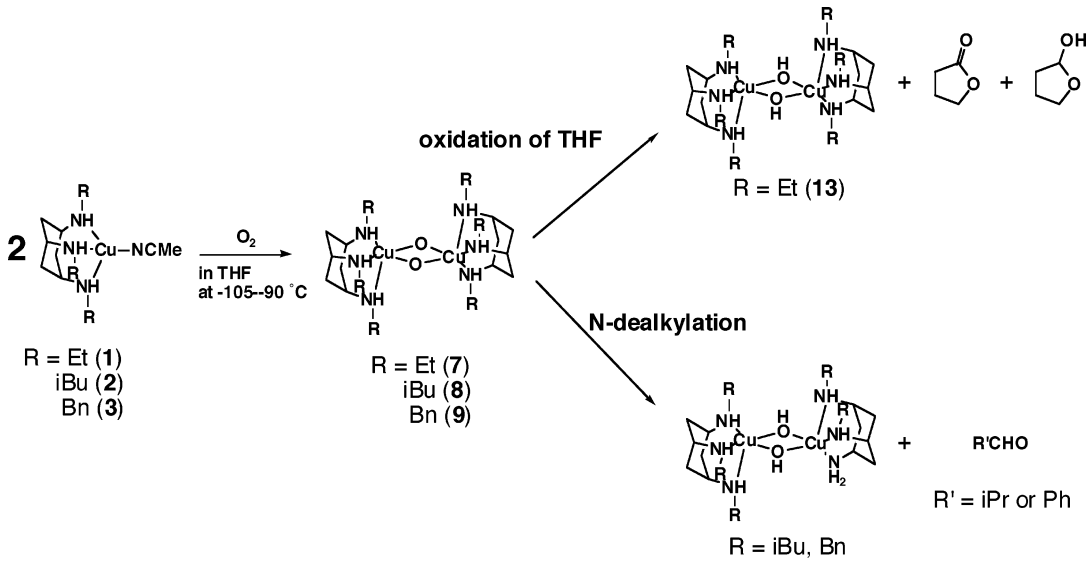

α-carbon of benzyl groups, which were abstracted by the activated oxide, may be located close to the μ-oxo anion as seen from the crystal structure of bis(μ-OH)dicopper(II) complex **12**. Thus, the thermal stability of **9** was the lowest among complexes **7**−**9**. The half-life measurements for **7** and **8** in CH_2Cl_2 were 1230 and 430 s, respectively. The half-life of **9** was too short to be evaluated. The thermal stability values of complexes **7**−**9** measured in CH_2Cl_2 were reduced relative to those measured in THF. This may be explained by the short distances between the amino hydrogen and μ-oxo oxygen. The $N_{eq}(H)\cdots O(H)$ distances estimated from the crystal structures of complexes **10**−**12** described previously were 2.727, 2.699, and 2.6702 Å, respectively. We suggest that if the structures of bis(μ-oxo)dicopper complexes **7**−**9** resemble the bis(μ-OH)dicopper complexes **10**−**12**, respectively, and $N_{eq}H\cdots O$ interactions are like hydrogen bonding, the differences in the thermal stabilities of complexes **7**−**9** in the two different solvents may arise from stronger $N_{eq}H\cdots O$ interactions occurring in CH_2Cl_2 than in THF. Furthermore, the THF molecule may be smaller and more likely to interact with Cu than CH_2Cl_2.

Bis(μ-oxo)dicopper complexes **8** and **9** were completely consumed at −80 °C in THF, and isobutylaldehyde and benzaldehyde were obtained as decomposition products in good yields of 31 and 32% (theoretical maximum 50%), respectively. The generation of isobutylaldehyde and benzaldehyde demonstrates that the α-carbons of iBu_3CY and Bn_3CY are hydroxylated to initiate the N-dealkylation process. Eyring plots and activation parameters for complexes **7**−**9** are shown in Figure 5 and Table 10, respectively. The activation parameters derived from the kinetic constants at various temperatures are $\Delta H^{\ddagger} = 34 \pm 2$ kJ mol^{-1} and $\Delta S^{\ddagger} = -114 \pm 9$ J K^{-1} mol^{-1} for **8** and $\Delta H^{\ddagger} = 30 \pm 1$ kJ mol^{-1} and $\Delta S^{\ddagger} = -104 \pm 6$ J K^{-1} mol^{-1} for **9**. The N-dealkylation rate constant for complex **9** at −90 °C was found to be 3.80×10^{-2} s^{-1}, which is 4 orders of magnitude higher than that of $[Cu_2(\mu\text{-}O)_2(Bn_3TACN)_2]^{2+}$ (1.6×10^{-6} s^{-1}), which was measured under the same reaction conditions as in CH_2Cl_2.[24] Complexes **8** and **9** exhibit higher N-dealkylation reactivity than $[Cu_2(\mu\text{-}O)_2(R_3TACN)_2]^{2+}$ (where R = iPr or Bn). In fact, N-dealkylation of **9** in CH_2Cl_2 occurred too quickly to measure the rate constant. The kinetic isotope effect (KIE)

Table 8. UV−vis and Resonance Raman Spectral Data for **7**−**9**

complex	solvent	λ_{max} (nm) (ϵ (M^{-1} cm^{-1}))	$\nu Cu-^{16}O$ (cm^{-1}) ($\nu Cu-^{18}O$ (cm^{-1}))	ref
7	THF	310 (15000), 411 (19000)	553, 581 (547)	this work
7	CH_2Cl_2	309 (15000), 408 (18000)		this work
d_{15}-**7**	THF	310 (15000), 411 (20000)		this work
d_{15}-**7**	CH_2Cl_2	311 (14000), 407 (18000)		this work
8	THF	316 (15000), 420 (19000)	571 (546)	40
8	CH_2Cl_2	321 (16000), 412 (19000)		this work
d_6-**8**	THF	318 (17000), 415 (20000)		this work
d_6-**8**	CH_2Cl_2	318 (17000), 412 (19000)		this work
Nd_3-**8**	THF	322 (16000), 420 (19000)		this work
Nd_3-**8**	CH_2Cl_2	316 (15000), 413 (18000)		this work
9	THF	306 (4600), 413 (4900)		this work
d_6-**9**	THF	308 (17000), 415 (23000)	585 (560)	this work
d_6-**9**	CH_2Cl_2	308 (17000), 413 (20000)		this work
$[Cu_2(\mu\text{-}O)_2(Me_3TACN)_2]^{2+a}$		307 (16000), 412 (18000)	604 (581)	20
$[Cu_2(\mu\text{-}O)_2(iPr_3TACN)_2]^{2+b}$		324 (11000), 448 (13000)	589 (567)	18, 19
$[Cu_2(\mu\text{-}O)_2(Bn_3TACN)_2]^{2+c}$		318 (12000), 430 (14000)	602, 612 (583)	17−19, 24
$[Cu_2(\mu\text{-}O)_2(Me_3TACD)_2]^{2+d}$		304 (16000), 404 (16000)	595 (575)	50
$[Cu_2(\mu\text{-}O)_2(Bn_3TACD)_2]^{2+e}$		312 (14000), 428 (14000)	600 (575)	50
$[Cu_2(\mu\text{-}O)_2(CD^{Me,Me})_2]^{2+f}$		301 (20000), 399 (25000)	605 (582)	20
$[Cu_2(\mu\text{-}O)_2(CD^{Me,Et})_2]^{2+g}$		306 (21000), 401 (28000)	610 (587)	20
$[Cu_2(\mu\text{-}O)_2(CD^{Et,Et})_2]^{2+h}$		319 (17000), 413 (23000)	616 (590)	20
$[Cu_2(\mu\text{-}O)_2(PD^{Me,Me})_2]^{2+i}$		297 (16000), 397 (24000)	609 (581)	31
$[Cu_2(\mu\text{-}O)_2(PD^{Me,Et})_2]^{2+j}$		305 (14000), 402 (23000)		14

[a] Me_3TACN: 1,4,7-trimethyl-1,4,7-triazacyclononane, in CH_2Cl_2. [b] iPr_3TACN: 1,4,7-triisopropyl-1,4,7-triazacyclononane. [c] Bn_3TACN: 1,4,7-tribenzyl-1,4,7-triazacyclononane, in CH_2Cl_2. [d] Me_3TACD: 1,5,9-trimethyl-1,5,9-triazacyclodecane, in CH_2Cl_2. [e] Bn_3TACD: 1,5,9-tribenzyl-1,5,9-triazacyclodecane, in CH_2Cl_2. [f] $CD^{Me,Me}$: *N*,*N*,*N*′,*N*′-tetramethyl-1*R*,2*R*-cyclohexanediamine, in CH_2Cl_2. [g] $CD^{Me,Et}$: *N*,*N*′-diethyl-*N*,*N*′-dimethyl-1*R*,2*R*-cyclohexanediamine, in CH_2Cl_2. [h] $CD^{Et,Et}$: *N*,*N*,*N*′,*N*′-tetraethyl-1*R*,2*R*-cyclohexanediamine, in CH_2Cl_2. [i] $PD^{Me,Me}$: *N*,*N*,*N*′,*N*′-tetramethyl-propanediamine, in CH_2Cl_2. [j] $PD^{Me,Et}$: *N*,*N*′-diethyl-*N*,*N*′-dimethyl-propanediamine, in CH_2Cl_2.

Table 9. Spontaneous Decomposition Rate Constants and Half-Life Times of **7**, d_{15}-**7**, **8**, d_6-**8**, Nd_3-**8**, **9**, and d_6-**9** at −90 °C

complex	**solvent**	k_{dec} (s^{-1})	**KIE (−90 °C)**	$\tau_{1/2}$ (s)
7	THF	2.78×10^{-4}	1.5	2490
	CH_2Cl_2	5.62×10^{-4}	2.1	1230
	THF-d_8	3.69×10^{-5}		18780
d_{15}-**7**	THF	1.84×10^{-4}		3770
	CH_2Cl_2	2.69×10^{-4}		2580
8	THF	8.04×10^{-4}	8.2	860
	CH_2Cl_2	1.62×10^{-3}	20	430
d_6-**8**	THF	9.79×10^{-5}		7080
	CH_2Cl_2	8.02×10^{-5}		8640
Nd_3-**8**	THF	1.11×10^{-3}		620
	CH_2Cl_2	1.30×10^{-3}3		530
9	THF	3.80×10^{-2}	45	18
d_6-**9**	THF	8.42×10^{-4}		820
	CH_2Cl_2	2.90×10^{-3}		240

values for **8**/d_6-**8** and **9**/d_6-**9** in THF were 8.2 and 45 at −90 °C, respectively, suggesting that the rate-determining step in the oxidative N-dealkylation is the abstraction of the α-carbon proton of the N-alkyl substituent. On the other hand, the activation parameters measured for the decomposition of **7** in THF were $\Delta H^{\ddagger} = 45 \pm 1$ kJ mol^{-1} and $\Delta S^{\ddagger} = -31 \pm 7$ J K^{-1} mol^{-1}, and the KIE value was 1.6 when d_{15}-**7** was used. The KIE value for **7** was smaller than the KIE values of **8** and **9**. These findings may indicate that the decomposition reaction of **7** includes oxidation of THF as an exogenous substrate. If **7** oxidizes THF, the decomposition rate of **7** in d_8-THF solution is expected to be reduced. In fact, the decomposition rate constant (3.69×10^{-5} s^{-1}) of **7** in d_8-THF was a lower value than that of **7** in THF (2.78×10^{-4} s^{-1}), and the KIE value was found to be 7.5. Product analysis of the decomposition reaction of **7** was performed using GC and GC/MS. As predicted, 2-hydroxytetrahydrofuran and γ-butyrolactone were detected as decomposition products of **7** in THF.[33,37,58] Acetaldehyde was not detected. The GC/MS chromatogram of the decomposition products of **7** is shown in Figure S5. The yields of 2-hydroxytetrahydrofuran and γ-butyrolactone were 25 and 3%, respectively, indicating that the THF molecule was oxygenated by the μ-oxo oxygen of **7**. The peaks of these compounds were obtained at *m*/*z* 87 and 86 (89 and 88 using $^{18}O_2$).[59] Interestingly, the Et_3CY ligand was almost completely recovered from the decomposition product of **7**. N-Dealkylation reaction decomposition products of **7** in CH_2Cl_2 were hardly observable in the ^1H NMR spectrum (Figure S6), indicating that the N-dealkylation reaction is not a major process causing the decomposition of **7**. The KIE value of **7** at −90 °C was found to be 2.1 (Table 9). This small KIE value also indicates that the N-dealkylation reaction is not a major process in the decomposition of **7** in CH_2Cl_2. However, we have not been able to reveal the decomposition mechanism of **7** in CH_2Cl_2.

For complexes **8** and **9** in CH_2Cl_2, the N-dealkylation reaction occurs to produce isobutylaldehyde and benzaldehyde, respectively. In contrast, **7** afforded a bis(μ-OH)-dicopper(II) complex (**13**). Fortunately, a single crystal of **13** was analyzed to obtain the crystal structure. The crystal parameters, molecular structure, and selected bond lengths and angles are given in Table 2, Figure 6, and Table 7,

(57) Taki, M.; Teramae, S.; Nagatomo, S.; Tachi, Y.; Kitagawa, T.; Itoh, S.; Fukuzumi, S. *J. Am. Chem. Soc.* **2002**, *124*, 6367−6377.
(58) Matsumoto, T.; Furutachi, H.; Kobino, M.; Tomii, M.; Nagatomo, S.; Tosha, T.; Osako, T.; Fujinami, S.; Itoh, S.; Kitagawa, T.; Suzuki, M. *J. Am. Chem. Soc.* **2006**, *128*, 3874−3875.
(59) In THF oxidation, primary isotope effects were observed as THF vs THF-d_8 and the transferred oxygen atom have been derived from the μ-oxo moiety. These findings suggest that THF oxidation to 2-hydroxytetrahydrofuran proceeds through a rebound-type mechanism similar to that of the reaction catalyzed by cytochrome *P*450.

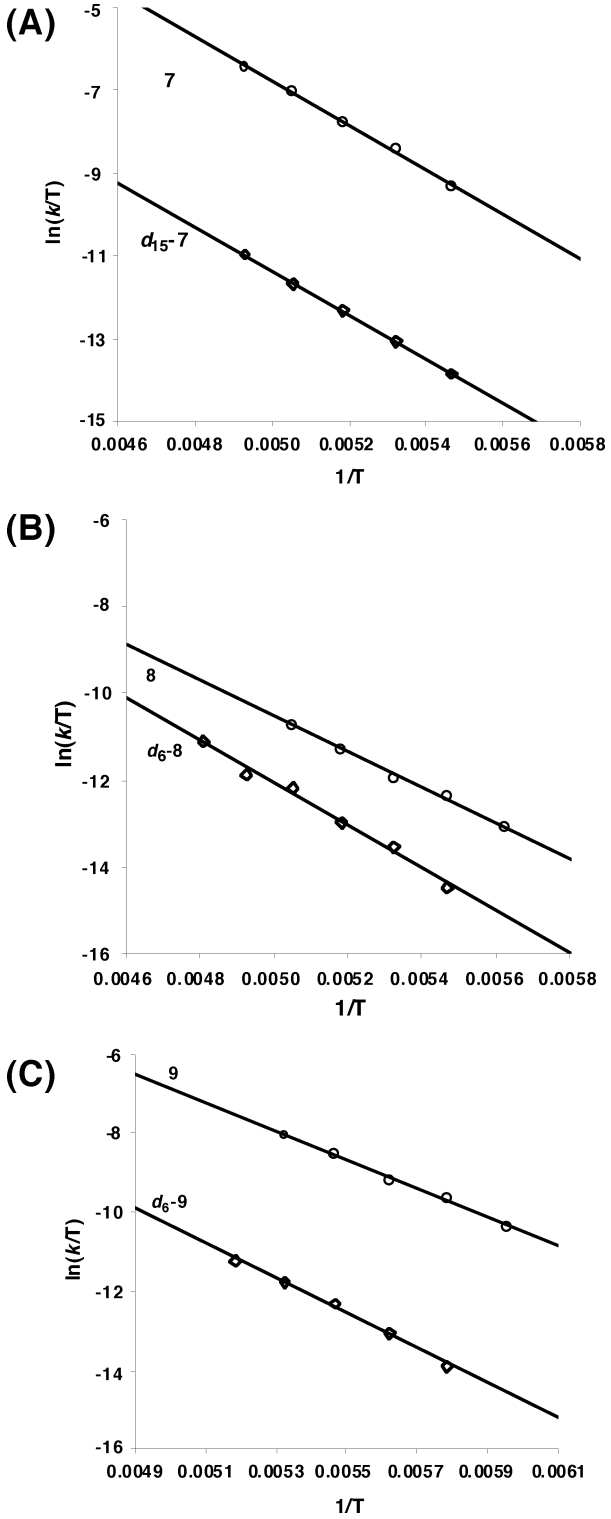

Figure 5. Eyring plots for the decompositions of $[Cu_2(R_3CY)_2(\mu\text{-}O)_2]^{2+}$ {R = Et (a), iBu (b), and Bn (c)} in THF.

respectively. One N−CH_2 group was fractionally disordered, and the structure indicates the atom pairs (C7, C8) and (C9, C10). This may suggest that the three ethyl groups can freely move around the metal center, which would in turn facilitate the approach of a THF molecule to the Cu_2O_2 center of **7**.

Electrostatic Interaction of N−H with μ-O Oxygen. As described previously, three bis(μ-oxo)dicopper(III) complexes with R_3CY have been characterized by identification

Table 10. Thermodynamic Parameters of **7**−**9**

complex/ligand	ΔH (kJ mol^{-1})	ΔS (J mol^{-1} K^{-1})	ref
7/Et_3CY (THF)	45 ± 1	−31 ± 7	this work
7/Et_3CY (CH_2Cl_2)	34 ± 2	−82 ± 8	this work
d_{15}-**7**/d_{15}-EtCY (THF)	44 ± 0.7	−71 ± 4	this work
d_{15}-**7**/d_{15}-EtCY (CH_2Cl_2)	26 ± 0.4	−166 ± 2	this work
8/iBu_3CY (THF)	34 ± 2	−114 ± 9	40
8/iBu_3CY (CH_2Cl_2)[a]	49 ± 2	−27 ± 9	this work
d_6-**8**/d_6-iBu_3CY (THF)	44 ± 1	−60 ± 6	this work
d_6-**8**/d_6-iBu_3CY (CH_2Cl_2)	49 ± 1	−15 ± 7	this work
9/Bn_3CY (THF)	30 ± 1	−104 ± 6	this work
d_6-**9**/d_6-Bn_3CY (THF)	37 ± 2	−100 ± 8	this work
d_6-**9**/d_6-Bn_3CY (CH_2Cl_2)	59 ± 2	33 ± 11	this work
Me_3TACN (CH_2Cl_2)	53 ± 2	−75 ± 4	20
iPr_3TACN (THF)	55 ± 2	−57 ± 5	24
d_{21}-iPr_3TACN (THF)	62 ± 2	−54 ± 5	24
Bn_3TACN (CH_2Cl_2)	58 ± 2	−41 ± 5	24
d_{21}-Bn_3TACN (CH_2Cl_2)	63 ± 2	−50 ± 5	24
$CD^{Me,Me}$ (CH_2Cl_2)	56 ± 2	−100 ± 4	20
$CD^{Me,Et}$ (CH_2Cl_2)	52 ± 2	−95 ± 4	20
$^{H}Py1^{Et,Bz}$ (CH_2Cl_2)[b]	55 ± 1	−31 ± 4	57
$^{Me}Py1^{Et,Bz}$ (CH_2Cl_2)[c]	31 ± 1	−121 ± 4	57
$^{H}Py1^{Et,Phe}$ (acetone)[d]	39.1 ± 0.4	−72.6 ± 1.9	21

[a] Activation parameters of **8** in CH_2Cl_2 were significantly different from those reported in ref 40. [b] $^{H}Py1^{Et,Bz}$: *N*-benzyl-*N*-ethyl-2-(2-pyridyl)ethylamine. [c] $^{Me}Py1^{Et,Bz}$: *N*-benzyl-*N*-ethyl-2-(6-methylpyridin-2-yl)ethylamine. [d] $^{H}Py1^{Et,Phe}$: *N*-ethyl-*N*-[2-(2-pyridyl)ethyl]-2-phenylethylamine.

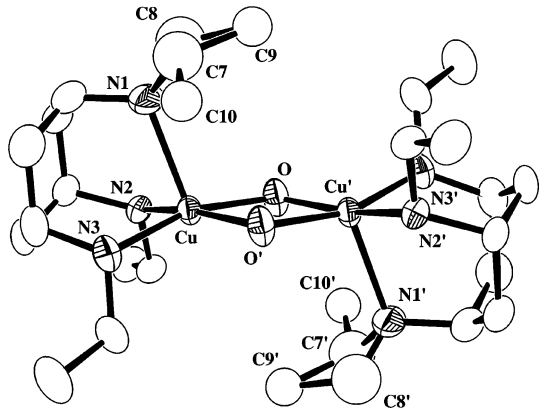

Figure 6. ORTEP view of the cationic portion of Cu(II) complex **13** with the atom numbering scheme (50% probability ellipsoids).

of higher O_2− activation via faster N-dealkylation reactions and oxidation of THF. The R_3CY ligands are secondary amines that have amino protons. The previously reported bis(μ-oxo)dicopper(III) complexes have supporting ligands consisting of tertiary amines and/or imines without N−H. The crystal structures of three $Cu_2(OH)_2$ complexes **10**−**12**, which have structures similar to the corresponding $Cu_2(O)_2$ complexes, are expected to have electrostatic interactions between the N−H group and the μ-oxo group of the $Cu_2(O)_2$ core.

To clarify these insights, we measured the isotope effect in kinetics experiments using **8** and clarified that **8** demonstrates the most unique hydroxylation reactivity among complexes **7**−**9**. The first-order rate constants for decomposition of the $Cu_2(O)_2$ complexes in CH_2Cl_2 at −90 °C were 1.62×10^{-3} s^{-1} for **8** and 1.30×10^{-3} s^{-1} for Nd_3-**8**, respectively (where all amino protons of iBu_3CY have been deuterated). The small KIE of 1.25 might suggest that N−H bond cleavage does not occur and that a weak electrostatic interaction between N−H hydrogen and μ-oxo oxygen has

Scheme 2

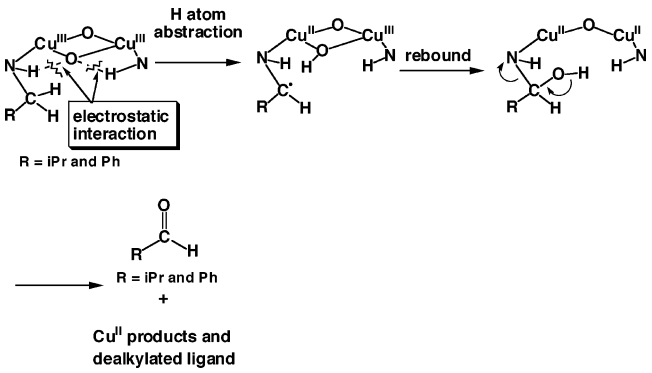

the major effect on the rate-determining step of decomposition. In the oxygenated form of myoglobin, a dioxygen storage protein found in muscle tissue, the distal histidine residue interacts with the oxygen molecule bound to heme. Small KIE values of 1.2 and 1.5 have been observed in the formation and dissociation processes of oxymyoglobin, respectively.[60] Similarly, the KIE values for dioxygen dissociation from oxyhemerythrin[61] are 1.55 for *Pseudomys gouldii* oxyhemerythrin,[60] 1.6 for *Themiste zostericola* oxymethemerythrin,[62] and 1.3 for *P. gouldii* oxymethemerythrin.[63] The hydrogen bond that forms when oxyhemerythrin releases dioxygen also contributes to the interactions between hydroperoxo hydrogen and μ-oxo oxygen of the Fe(III)−O−Fe(III) core.[64] Taking these facts into consideration, the small KIE value of 1.25 for **8** is appropriate.[65] The small KIE value for **8** must suggest that the electrostatic interaction between N−H and μ-oxo oxygen influences the oxidation ability of the $Cu_2(O)_2$ species. Cytochrome *c* peroxidase from yeast is known to form an Fe(IV)═O porphyrin π-cation radical metal oxo species in the enzymatic reaction, and the N−H groups of Trp 191 and Arg 48 are located close to the oxygen atom of Fe(IV) ═O at distances of 2.6−3.0 Å.[66] These observations suggest a mechanism of oxygenation of hydrocarbons by complexes **7**−**9** as follows: (i) the N−H proton interacts electrostatically with the μ-oxo oxygen of the $Cu(III)_2(\mu\text{-}O)_2$ core, (ii) the μ-oxo oxygen abstracts a hydrogen atom from the hydrocarbon to produce a carbon radical as soon as the interaction weakens, and (iii) the carbon radical reacts with the hydroxyl radical bound to the dicopper center to produce the corresponding oxidative product. The proposed decomposition mechanisms of **8** and **9** are shown in Scheme 2. Thus, it is possible for a high-valent metal oxo species to promote the oxygenation of hydrocarbons more effectively via a weak electrostatic interaction with functional groups containing a polarized hydrogen atom such as amino and alcohol groups.

Conclusion

We synthesized three copper(I) complexes (complexes **1**−**3**) with R_3CY (R = Et, iBu, and Bn) ligands containing a secondary amine as a coordinating ligand atom. Three corresponding carbonyl complexes, **4**−**6**, were also prepared. Exposure of **1**−**3** to dioxygen afforded the corresponding bis(μ-oxo)dicopper(III) complexes (complexes **7**−**9**) in THF or in CH_2Cl_2 in the range of −105 to −80 °C. Resonance Raman spectra for complexes **7**, **8**, and d_6-**9** exhibited Cu−O stretching vibrations at 553/581, 571, and 585 cm^{-1}, respectively, which are lower in energy than those of previously reported bis(μ-oxo)dicopper(III) complexes. These observations may be attributed to the six-membered chelate ring of R_3CY and/or an electrostatic interaction of the N−H group of R_3CY with the bridging μ-oxo in the $Cu(III)_2(\mu\text{-}O)_2$ core. In THF solvent, bis(μ-oxo)dicopper(III) complexes **8** and **9** oxidized their ligands via an intramolecular mechanism resulting in N-dealkylation of isobutylaldehyde for **8** and benzaldehyde for **9**. On the other hand, in THF solvent, complex **7** oxidized a THF molecule as an exogenous substrate. These results are rationalized as follows: the steric repulsion at the Cu_2O_2 center of **7** is smaller than the steric repulsion at the Cu_2O_2 center of compounds **8** and **9**. Thus, exogenous substrates can easily approach the Cu_2O_2 center of complex **7**. The decomposition reaction of **8** was investigated in detail by kinetic measurements. A small kinetic isotope effect was observed (KIE = 1.25), indicating that a weak electrostatic interaction exists between N−H and μ-oxo in the $Cu(III)_2(\mu\text{-}O)_2$ core. These findings suggest that the electrostatic interaction of a polarized N−H proton with the metal−oxo oxygen increases the oxidative reactivity of the metal−oxo species.

Acknowledgment. We gratefully acknowledge support for this work from a Grant-in-Aid for Scientific Research from the Ministry of Education, Science, Sports and Culture and in part by a grant from the NITECH 21st Century COE Program.

Supporting Information Available: X-ray crystallographic data files in CIF format for **1**−**3**, **6**, and **10**−**13**. Tables S1−S72, crystallographic experimental details, final atomic coordinates, thermal parameters, full bond lengths and angles, ORTEP drawings, and full cells for **1**−**3**, **6**, and **10**−**13**. Figure S1, the cyclic voltammograms of **1**−**3**. Figures S2−S4, UV−vis, resonance Raman spectra, and first-order plots of complexes **7**−**9**. Figure S5, GC/MS data for products obtained from a decomposition reaction of **7** in THF. Figure S6, ^{1}H NMR spectra of a product obtained from decomposition of **7** in CH_2Cl_2. This material is available free of charge via the Internet at http://pubs.acs.org.

IC062206S

(60) Armstrong, G. D.; Sykes, A. G. *Inorg. Chem.* **1986**, *25*, 3135−3139.
(61) Stenkamp, R. E. *Chem. Rev.* **1994**, *94*, 715−726.
(62) Lloyd, C. R.; Eyring, E. M.; Ellis, W. R., Jr. *J. Am. Chem. Soc.* **1995**, *117*, 11993−11994.
(63) Xiong, J.; Phillips, R. S.; Kurtz, D. M., Jr.; Jin, S.; Ai, J.; Sanders-Loehr, J. *Biochemistry* **2000**, *39*, 8526−8536.
(64) Kryatov, S. V.; Rybak-Akimova, E. V.; Schindler, S. *Chem. Rev.* **2005**, *105*, 2175−2226.
(65) Fulop, V.; Phizackerley, R. P.; Soltis, S. M.; Clifton, I. J.; Wakatsuki, S.; Erman, J.; Hajdu, J.; Edwards, S. L. *Structure* **1994**, *2*, 201−208.